cells and additive effects in WiDr cells. Sequential exposure to pemetrexed for 24 h followed by paclitaxel showed synergistic effects in A549 and MCF7 cells and additive effects in PA1 and WiDr cells. However, the combined data points in PA1 and WiDr cells were close to the borderlines between supraadditive and additive areas (Fig. 4), and the observed data were close to the predicted minimum values for an additive effect (Table 1). The combined data points in WiDr cells fell both in the area of supraadditivity and within the envelope of additivity (Fig. 4). Since the isobologram of Steel and Peckham is more strict for synergism and antagonism than other methods for evaluating the effects of drug combinations, simultaneous exposure to pemetrexed and paclitaxel and sequential exposure to pemetrexed followed by paclitaxel would be defined as having antagonistic and synergistic effects, respectively, using other methods.

On the other hand, sequential exposure to paclitaxel followed by pemetrexed showed additive effects in all four cell lines tested. The results of flow cytometric analysis of PA1 cells were consistent with these findings. Enhanced apoptosis was observed only in the pemetrexed–paclitaxel sequence (data not shown).

Our findings suggest that the simultaneous administration of pemetrexed and paclitaxel on the same day is convenient for clinical use but is suboptimal. The sequential administration of pemetrexed followed by paclitaxel may be the optimal schedule for these combinations. For example, administrations of pemetrexed on day 1 and paclitaxel on day 2 would be worthy of clinical investigation. Several in vitro and in vivo studies of combinations of pemetrexed with paclitaxel have been reported [28, 34, 35]. Schultz et al. observed synergistic effects when pemetrexed exposure preceded paclitaxel exposure by 24 h, while the reverse order produced only additive effects in three human cancer cells in vitro [28]. Although the detailed experimental systems are not described in the abstract, our data support their findings.

Teicher et al. studied the combination of pemetrexed and paclitaxel in vivo against EMT-6 murine mammary carcinoma using a tumor cell survival assay [34]. They observed that pemetrexed administered four times over 48 h with paclitaxel administered with the third dose of pemetrexed produced an additive or more than additive tumor response. They further studied the combination of pemetrexed and paclitaxel in human tumor xenografts [35]. Administration of pemetrexed (days 7–11, days 14–18) along with paclitaxel (days 8, 10, 12, and 15) produced greater-than-additive effects on human lung cancer H460 tumor growth delay, while that of pemetrexed (days 7–11) along with paclitaxel (days 7, 9, 11, and 13) produced additive effects on human breast cancer MX-1 tumor growth delay. Since the schedules of administration of pemetrexed with paclitaxel were quite different from ours, comparison seems difficult.

The mechanisms underlying the schedule-dependent synergism and antagonism of the combination of pemetrexed and paclitaxel are unclear. Cell cycle analysis showed that initially exposing cells to pemetrexed leads to synchronization in the S phase (data not shown). Cells in the S phase are sensitive to paclitaxel, in addition to cells in $G_2$/M phase [17]. This may explain the synergistic effects of sequential exposure to pemetrexed followed by paclitaxel. Simultaneous exposure to pemetrexed and paclitaxel produced antagonistic effects. Pemetrexed has a cytotoxic effect by blocking cells in the S phase [38], while paclitaxel has cytotoxic effects by blocking cells in the $G_2$/M phase [17, 27]. Thus, one agent might reduce the cytotoxicity of the other agent by preventing cells from entering the specific phase in which the cells are most cytotoxic to the other agent. Interestingly, we have observed similar cytotoxic interactions between methotrexate and paclitaxel [15]. Simultaneous exposure to methotrexate and paclitaxel produces antagonistic effects, while the methotrexate/paclitaxel sequence produces synergistic effects and the reverse sequence produces additive effects. These experimental data suggest that antifolates, which inhibit dihydrofolate reductase, may enhance the cytotoxic action of paclitaxel in sequential administration.

It should be noted that in vitro studies cannot evaluate toxic and pharmacokinetic interactions. Thus, in vivo studies are required to confirm whether the pemetrexed–paclitaxel sequence is optimal or not. In clinical oncology, drug interaction may result in synergism, not only in terms of efficacy but also in terms of toxic side effects. If the toxicities of the drug combinations were compared between the schedules of synergistic and antagonistic interactions at the same doses, the schedules with antagonistic interactions may produce less toxicity than the schedules with synergistic interactions. Our data showed that the drug doses required for $IC_{80}$ or $IC_{50}$ levels with sequential exposure to pemetrexed followed by paclitaxel are less than 70% of the drug doses required for $IC_{80}$ or $IC_{50}$ with simultaneous exposure to the two agents (Figs. 3 and 4). This suggests that the optimal doses for sequential administration of pemetrexed followed by paclitaxel may be lower than those for the simultaneous administration of the two agents. This is important and must be kept in mind for translating in vitro data to clinical applications, since the schedule showing antagonistic effects of the combination may be selected because of less toxicity during the first stage of clinical study.

In conclusion, our findings suggest that the cytotoxic effects of the combination of pemetrexed and paclitaxel are schedule-dependent. The optimal schedule of pemetrexed in combination with paclitaxel is the sequential administration of pemetrexed followed by paclitaxel. Although there are a number of difficulties in the translation of results from in vitro to clinical therapy, this schedule should be assessed in clinical trials for the treatment of solid tumors.

**Acknowledgments** This work was supported in part by a Grant-in-Aid for Cancer Research (11-8) from the Ministry of Health and Welfare and by a Grant-in-Aid for Research on the Second-Term

Comprehensive 10-Year Strategy for Cancer Control from the Ministry of Health and Welfare of Japan.

## References


1. Arbuck SG (1995) Paclitaxel: current developmental approaches of the National Cancer Institute. Semin Oncol 22:55–56
2. Britten CD, Izbicka E, Hilsenbeck S, Lawrence R, Davidson K, Cerna C, Gomez L, Rowinsky EK, Weitman S, Van Hoff DD (1999) Activity of the multitargeted antifolate MTA in the human tumor cloning assay. Cancer Chemother Pharmacol 44:105–110
3. Calvert AH, Walling JM (1998) Clinical studies with MTA. Br J Cancer 78 [Suppl 3]:35–40
4. Celio L, Buzzoni R, Longarini R, Marchiano A, Bajetta E (2002) Pemetrexed in gastric cancer: clinical experience and future perspectives. Semin Oncol 29 [Suppl 18]:63–68
5. Chen VJ, Bewley JR, Smith PG, Andis SL, Schultz RM, Iversen PW, Tonkinson JL, Shih C (2000) An assessment of the antithymine and antipurine characteristics of MTA (LY231514) in CCRF-CEM cells. Adv Enzyme Regul 40:143–154
6. Donehower RC, Rowinsky EK (1993) An overview of experience with taxol (paclitaxel) in the USA. Cancer Treat Rev 19 [Suppl C]:63–78
7. Habeck LL, Mendelsohn LG, Shih C, Taylor EC, Colman PD, Gossett LS, Leitner TA, Schultz RM, Andis SL, Moran RG (1995) Substrate specificity of mammalian folypolyglutamate synthetase for 5,10-dideazatetrahydrofolate analogs. Mol Pharmacol 48:326–333
8. Haller DG (2002) Future directions in the treatment of pancreatic cancer. Semin Oncol 29 [Suppl 20]:31–39
9. Hanauske AR, Chen V, Paoletti P, Niyikiza C (2001) Pemetrexed disodium: a novel antifolate clinically active against multiple solid tumors. Oncologist 6:363–373
10. Hochster H (2002) The role of pemetrexed in the treatment of colorectal cancer. Semin Oncol 29 [6 Suppl 18]:54–56
11. Kano Y, Ohnuma T, Okano T, Holland JF (1988) Effects of vincristine in combination with methotrexate and other antitumor agents in human acute lymphoblastic leukemia cells in culture. Cancer Res 48:351–356
12. Kano Y, Sakamoto S, Kasahara T, Akutsu M, Inoue Y, Miura Y (1991) In vitro effects of amsacrine in combination with other anticancer agents. Leuk Res 15:1059–1064
13. Kano Y, Akutsu M, Tsunoda S, Ando J, Matsui J, Suzuki K, Ikeda T, Inoue Y, Adachi K (1996) Schedule-dependent interaction between paclitaxel and 5-fluorouracil in human carcinoma cell lines in vitro. Br J Cancer 74:704–710
14. Kano Y, Akutsu M, Tsunoda S, Suzuki K, Adachi K (1998) In vitro schedule-dependent interaction between paclitaxel and SN-38 (the active metabolite of irinotecan) in human carcinoma cell lines. Cancer Chemother Pharmacol 42:91–98
15. Kano Y, Akutsu M, Tsunoda S, Furuta M, Yazawa Y, Ando J (1998) Schedule-dependent synergism and antagonism between paclitaxel and methotrexate in human carcinoma cell lines. Oncol Res 10:347–354
16. Kano Y, Akutsu M, Tsunoda S, Mano H, Sato Y, Honma Y, Furukawa Y (2001) In vitro cytotoxic effects of a tyrosine kinase inhibitor STI571 in combination with commonly used antileukemic agents. Blood 97:1999–2007
17. Lieu CH, Chang YN, Lai YK (1997) Dual cytotoxic mechanisms of submicromolar taxol on human leukemia HL-60 cells. Biochem Pharmacol 53:1587–1596
18. McDonald AC, Vasey PA, Adams L, Walling J, Woodworth JR, Abrahams T, McCarthy S, Bailey NP, Siddiqui N, Lind MJ, Calvert AH, Twelves CJ, Cassidy J, Kaye SB (1998) A phase I and pharmacokinetic study of LY231514, the multitargeted antifolate. Clin Cancer Res 4:605–610
19. O'Shaughnessy JA, Gennari A, Conte P (2002) Pemetrexed: a promising new treatment for breast cancer. Semin Oncol 29 [2 Suppl 5]:36–41
20. Paz-Ares L, Ciruelos E, Garcia-Carbonero R, Castellano D, Lopez-Martin A, Cortes-Funes H (2002) Pemetrexed in bladder, head and neck, and cervical cancers. Semin Oncol 29 [Suppl 18]:69–75
21. Paz-Ares L, Bezares S, Tabernero JM, Castellanos D, Cortes-Funes H (2003) Review of a promising new agent—pemetrexed disodium. Cancer [Suppl] 97:2056–2063
22. Raymond E, Louvet C, Tournigand C, Coudray AM, Faivre S, De Gramont A, Gespach C (2002) Pemetrexed disodium combined with oxaliplatin, SN38, or 5-fluorouracil, based on the quantitation of drug interactions in human HT29 colon cancer cells. Int J Oncol 21:361–367
23. Rinaldi DA (1999) Overview of phase I trials of multitargeted antifolate (MTA, LY231514). Semin Oncol 26 [Suppl 6]:82–88
24. Rinaldi DA, Burris HA, Dorr FA, Woodworth JR, Kuhn JG, Eckardt JR, Rodriguez G, Corso SW, Fields SM, Langley C, Clark G, Faries D, Lu P, Van Hoff DD (1995) Initial phase I evaluation of the novel thymidylate synthase inhibitor, LY231514, using the modified continual reassessment method for dose escalation. J Clin Oncol 13:2842–2850
25. Rinaldi DA, Kuhn JG, Burris HA, Dorr FA, Rodriguez G, Eckhardt SG, Jones S, Woodworth JR, Baker S (1999) A phase I evaluation of multitargeted antifolate (MTA, LY231514), administered every 21 days, utilizing the modified continual reassessment method for dose escalation. Cancer Chemother Pharmacol 44:372–380
26. Scagliotti GV, Shin DM, Kindler HL, Vasconcelles MJ, Keppler U, Manegold C, Burris H, Gatzemeier U, Blatter J, Symanowski JT, Rusthoven JJ (2003) Phase II study of pemetrexed with and without folic acid and vitamin $B_{12}$ as front-line therapy in malignant pleural mesothelioma. J Clin Oncol 21:1556–1561
27. Schiff PB, Fant J, Horwitz SB (1979) Promotion of microtubule assembly in vitro by taxol. Nature 277:665–667
28. Schultz RM, Dempsey JA, Kraus LA, Schmid SM, Calvete JA, Laws AL (1999) In vitro sequence dependence for the multitargeted antifolate (MTA, LY231514) combined with other anticancer agents. Eur J Cancer 35 [Suppl 4]:S194
29. Shih C, Thornton DE (1998) Preclinical pharmacology studies and the clinical development of a novel multitargeted antifolate, MTA (LY231514). In: Jackman AL (ed) Anticancer drug development guide: antifolate drugs in cancer therapy. Humana, Totowa, p 183
30. Shih C, Chen VJ, Gossett LS, Gates SB, MacKellar WC, Habeck LL, Shackelford KA, Mendelsohn LG, Soose DJ, Patel VF, Andis SL, Bewley JR, Rayl EA, Moroson BA, Beardsley GP, Kohler W, Ratnam M, Schultz RM (1997) LY231514, a pyrrolo[2,3-d]pyrimidine-based antifolate that inhibits multiple folate-requiring enzymes. Cancer Res 57:1116–1123
31. Shih C, Habeck LL, Mendelsohn LG, Chen VJ, Schultz RM (1998) Multiple folate enzyme inhibition: mechanism of a novel pyrrolopyrimidine-based antifolate LY231514 (MTA). Adv Enzyme Regul 38:135–152
32. Steel GG, Peckham MJ (1979) Exploitable mechanisms in combined radiotherapy–chemotherapy: the concept of additivity. Int J Radiat Oncol Biol Phys 5:85–91
33. Taylor EC, Kuhnt D, Shih C, Rinzel SM, Grindey GB, Barredo J, Jannatipour M, Moran RG (1992) A dideazatetrahydrofolate analogue lacking a chiral center at C-6, *N*-[4-[2-(2-amino-3,4-dihydro-4-oxo-7H-pyrrolo[2,3-d]pyrimidin-5-yl)ethyl]benzoyl]-L-glutamic acid, is an inhibitor of thymidylate synthase. J Med Chem 35:4450–4454
34. Teicher BA, Alvarez E, Liu P, Lu K, Menon K, Dempsey J, Schultz RM (1999) MTA (LY231514) in combination treatment regimens using human tumor xenografts and the EMT-6 murine mammary carcinoma. Semin Oncol 28:55–62
35. Teicher BA, Chen V, Shih C, Menon K, Forler PA, Phares VG, Amsrud T (2000) Treatment regimens including the multitargeted antifolate LY231514 in human tumor xenografts. Clin Cancer Res 6:1016–1023

36. Tesei A, Ricotti L, De Paola F, Amadori D, Frassineti GL, Zoli W (2002) In vitro schedule-dependent interactions between the multitargeted antifolate LY231514 and gemcitabine in human colon adenocarcinoma cell lines. Clin Cancer Res 8:233–239
37. Tomek S, Emri S, Krejcy K, Manegold C (2003) Chemotherapy for malignant pleural mesothelioma: past results and recent developments. Br J Cancer 88:167–174
38. Tonkinson JL, Marder P, Andis SL, Schultz RM, Gossett LS, Shih C, Mendelsohn LG (1997) Cell cycle effects of antifolate antimetabolites: implications for cytotoxicity and cytostasis. Cancer Chemother Pharmacol 39:521–531
39. Vogelzang NJ, Rusthoven JJ, Symanowski J, Denham C, Kaukel E, Ruffie P, Gatzemeier U, Boyer M, Emri S, Manegold C, Niyikiza C, Paoletti P (2003) Phase III study of pemetrexed in combination with cisplatin versus cisplatin alone in patients with malignant pleural mesothelioma. J Clin Oncol 21:2636–2644

[Cancer Biology & Therapy 3:1, 96-101. January 2004]; ©2004 Landes Bioscience

Research Paper

# The Tyr-Kinase Inhibitor AG879, That Blocks the ETK-PAK1 Interaction, Suppresses the RAS-Induced PAK1 Activation and Malignant Transformation

**Hong He**[1]
**Yumiko Hirokawa**[1]
**Aviv Gazit**[2]
**Yoshihiro Yamashita**[3]
**Hiroyuki Mano**[3]
**Yuko Kawakami**[4]
**Kawakami**[4]
**Ching-Yi Hsieh**[5]
**Hsing-Jien Kung**[5]
**Guillaume Lessene**[6]
**Jonathan Baell**[6]
**Alexander Levitzki**[2]
**Hiroshi Maruta**[1,*]

[1]Ludwig Institute for Cancer Research; Royal Melbourne Hospital; Parkville/Melbourne, Australia

[2]Department of Biological Chemistry; The Alexander Silverman Institute of Life Sciences; Hebrew University of Jerusalem; Jerusalem, Israel,

[3]Division of Functional Genomics; Jichi Medical School; Tochigi, Japan

[4]La Jolla Institute for Allergy and Immunology; San Diego, California USA

[5]Cancer Center; University of California at Davis; Sacramento, California USA

[6]Walter and Eliza Hall Institute for Medical Research; Parkville/Melbourne, Australia

*Correspondence to: Hiroshi Maruta; Ludwig Institute for Cancer Research; P.O. Box 2008 Royal Melbourne Hospital; Parkville/Melbourne, Australia 3050; Tel.: 613.9341.3155; Fax: 613.9341.3104; Email: Hiroshi.maruta@ludwig.edu.au

Received 09/16/03; Accepted 10/29/03

Previously published online as a *Cancer Biology & Therapy* E-publication: http://www.landesbioscience.com/journals/cbt/abstract.php?id=643

## KEY WORDS

AG879, ETK, RAS, PAK, transformation

## ACKNOWLEDGEMENTS

We thank Mrs. Thao Nheu and Dr. Hong-jian Zhu for their generous gift of a doxycycline-inducible RAS transformant of NIH/3T3 cells; Dr. Yun Qiu for her generous gift of the ETK PH domain construct in a pGEX vector; Dr. Nathan Hall for his comparison of the 3D structure of the kinase domain between ETK, BTK and TEC by a molecular modelling; and Prof. Tony Burgess for his consistent support and advice throughout this work.

## ABSTRACT

AG 879 has been widely used as a Tyr kinase inhibitor specific for ErbB2 and FLK-1, a VEGF receptor. The $IC_{50}$ for both ErbB2 and FLK-1 is around 1 μM. AG 879, in combination of PP1 (an inhibitor specific for Src kinase family), suppresses almost completely the growth of RAS-induced sarcomas in nude mice. In this paper we demonstrate that AG 879 even at 10 nM blocks the specific interaction between the Tyr-kinase ETK and PAK1 (a CDC42/ Rac-dependent Ser/Thr kinase) in cell culture. This interaction is essential for both the RAS-induced PAK1 activation and transformation of NIH 3T3 fibroblasts. However, AG 879 at 10 nM does not inhibit either the purified ETK or PAK1 directly in vitro, suggesting that this drug blocks the ETK-PAK1 pathway by targeting a highly sensitive kinase upstream of ETK. Although the Tyr-kinases Src and FAK are known to activate ETK directly, Src is insensitive to AG 879, and FAK is inhibited by 100 nM AG 879, but not by 10 nM AG879. The structure-function relationship analysis of AG 879 derivatives has revealed that both thio and tert-butyl groups of AG 879, but not (thio) amide group, are essential for its biological function (blocking the ETK-PAK1 pathway), suggesting that through the (thio) amide group, AG 879 can be covalently linked to agarose beads to form a bioactive affinity ligand useful for identifying the primary target of this drug.

## INTRODUCTION

PAK1, a member of CDC42/Rac-dependent Ser/Thr kinase family (PAKs), is activated by oncogenic RAS mutants such as v-Ha-RAS, and is essential for RAS-transformation of fibroblasts such as Rat-1 and NIH 3T3 cells.[1,2] Several distinct pathways appear to be essential for v-Ha-RAS-induced activation of PAK1 in these cells.[2] One of these pathways involves PI-3 kinase which produces phosphatidyl-inositol 3,4,5 trisphosphate (PIP3) that activates both CDC42 and Rac GTPases through a GDP-dissociation stimulator (GDS) called VAV. A second pathway involves PIX, an SH3 protein which binds a Pro-rich motif (residues 186-203, PAK18) located between the N-terminal GTPase-binding domain and C-terminal kinase domain of PAK1.[3] PIX binds another protein called CAT which is a substrate of Src family kinases.[4] A third pathway involves an SH2/SH3 adaptor protein called NCK.[5] The SH3 domain of NCK binds another Pro-rich motif of PAK1 located near the N-terminus, while the SH2 domain of NCK binds the Tyr-phosphorylated EGF receptor/ErbB1.[5] Thus, when ErbB1 is activated by EGF, PAK1 is translocated to the plasma membrane through NCK. The involvement of both Src family kinases and ErbB1 in the PAK1 activation is also supported by our finding that both PP1 (inhibitor of Src family kinases) and AG1478 (ErbB1-specific inhibitor) block the RAS-induced PAK1 activation and transformation in vitro and in vivo.[2,6] A fourth pathway involves ErbB2, a member of ErbB family Tyr kinases.[2] We have previously shown that AG 825 (ErbB2-specific inhibitor) blocks RAS-induced activation of PAK1 and malignant transformation with the $IC_{50}$ around 0.35 μM.[2] A fifth pathway has been recently discovered in which RAS activates PAK1 through Tiam1, a Rac-specific GDS , in a PI-3 kinase-independent manner.[7] In this pathway, RAS directly binds Tiam1 which in turn activates Rac.[7]

Another possible pathway involves β1-integrin, FAK and ETK. β1-integrin activates the Tyr kinase FAK, which in turn phosphorylates and activates ETK,[8] a member of TEC/BTK family Tyr kinases.[9,10] ETK carries an N-terminal pleckstrin homology (PH) domain followed by a TEC homology domain.[9,10] Activated ETK binds PAK1 through the PH domain, phosphorylates and activates PAK1.[11] However, it still remains to be

clarified (1) whether RAS requires this integrin/FAK/ ETK pathway for its oncogenicity, and (2) how RAS activates this pathway.

To suppress the growth of RAS-induced sarcomas in vivo (in nude mice), we previously used AG 879, a Tyr-kinase inhibitor specific for ErbB2 and VEGF receptor FLK-1.[2,12,13] In this paper we demonstrate that AG879 inhibits selectively the activation of ETK ($IC_{50}$ around 5 nM), blocking RAS-induced ETK-mediated activation (Tyr phosphorylation) of PAK1 to suppress RAS transformation.

## MATERIALS AND METHODS

**Cell Culture and Reagents.** v-Ha-RAS-transformed NIH 3T3 fibroblasts (RAS cells) were grown in a standard medium, i.e., Dulbecco's modified Eagle's medium in the presence or absence of 10% fetal calf serum as described previously.[2,6] The Tyr kinase inhibitor AG879 and its derivatives (AG 306 and AG 1584 ) were synthesized as described previously.[12] The novel derivative GL-2002 was synthesized analogously, and full synthetic details will be published in due course. Two other AG 879 derivatives (AG 99 and AG 213) were purchased from Calbiochem (Croydon, Australia). The following antibodies were obtained from Santa Cruz Biotechnology (Santa Cruz,CA): anti-PAK1 antibody, anti-phospho-Tyr antibody (PY99) and goat-anti-ETK antibody. The rabbit anti-FAK antibody was a generous gift of Dr. David Schlaepfer (The Scripps Research Institute, La Jolla, CA). The mouse anti-ETK antibody was purchased from Becton Dickinson Biosciences (North Ryde, NSW, Australia). The rabbit anti-ETK antibody was prepared as described previously.[14]

**Assay for the Effect of AG 879 on Cell Growth.** The effect of AG879 on anchorage-independent growth of RAS cells was determined by seeding $10^3$ cells per plate into 0.35% top agar containing different concentrations of AG879 (from 1 nM to 1 μM) and incubating for 3 weeks as described previously.[2,6,15] At the end of 3 weeks, the colonies formed in the agar were stained and counted. The effect of AG 879 on anchorage-dependent growth of RAS cells and normal NIH/3T3 fibroblasts was examined by seeding $10^3$ cells per plate in the medium containing 1–100 nM AG 879, incubating for 5 days and counting as described previously.[2,6,15]

**PAK and ETK Kinase Assays.** For the PAK kinase assay, RAS cells were serum-starved overnight, and then treated with different concentrations of AG879 for 1 hour as described in the text. The cells were lysed in the lysis buffer (40 mM HEPES, pH 7.4, 1% Nonidet P-40, 1 mM EDTA, 100 mM NaCl, 25 mM NaF, 100 μM $NaVO_3$, 1 mM phenylmethylsulfonyl fluoride (PMSF), and 100 units/ml aprotinin). The lysates containing 1 mg of proteins (measured by Bradford assay) were immuno-precipitated with the anti-PAK1 antibody, and the immuno-precipitates were subjected to the PAK kinase assay as described previously.[1,2,6,16] The direct effect of AG 879 on PAK1 was determined in vitro, using GST-PAK1 fusion protein as described previously.[17] For ETK kinase assay, serum-starved RAS cells were lysed in a buffer containing 20 mM Tris-HCl (pH 7.5), 100 mM NaCl, 10% glycerol, 1% Nonidet P-40, 10 mM NaF, 100 μM $NaVO_3$, 1 mM PMSF, and 100 units/ml aprotinin. The cell lysates were immuno-precipitated with the rabbit anti-ETK antibody, and the ETK kinase assay was performed as described previously[8,11] using the endogenous PAK1 associated with ETK as a substrate in the presence or absence of different concentrations of AG879 or its derivatives such as AG 1584. Immuno-blotting was performed to determine the protein levels for PAK1 and ETK (see below).

**Immuno-Precipitation and Immuno-Blotting.** Serum-starved RAS cells were treated with different concentrations of AG879 as indicated in the text. The cells were lysed in two different lysis buffers mentioned above. The cell lysates containing 1.5–2.0 mg of protein (measured by Bradford assay) were incubated with protein A-Sepharose beads (Amersham Pharmacia Biotech) and anti-PAK1, anti-ETK or anti-FAK antibodies separately.[2,8,11,18] The proteins in immuno-precipitates were separated on 4–12% NuPage gel (Invitrogen) electrophoresis and transferred to a nitrocellulose membrane (Micron Separations, Inc.). The membranes were blocked with 10% (w/v) skim milk in phosphate-buffered saline containing 0.04% Tween20 (PBST), followed by an incubation for 1 hr at room temperature with different first antibodies as described in the text. After washing with PBST, the blots were incubated with horseradish peroxidase-conjugated anti-mouse or anti-rabbit (Bio-Rad) secondary antibodies. The bound antibodies were visualised using ECL reagents (Amersham Pharmacia Biotech). Some membranes were stripped and reblotted[19] with different antibodies as described in the text.

**The ETK Baculo Viral Construct and its Affinity-Purification.** The plasmid encoding the full-length ETK (residues 1-674)[14] was constructed in pBacPAK8 transfer vector (Clontech, Palo Alto, CA) and recombinant virus was made by Dr. Chi-Ying F. Huang (NHRI, Taiwan). Sf9 insect cells infected with the recombinant virus were harvested and disrupted with ice-cold lysis buffer containing 10 mM Tris pH, 7.5; 130 mM NaCl; 1% Triton X-100; 10 mM NaF; 10 mM Na phosphate; 10 mM Na pyro-phosphate and protease inhibitor cocktail (Pharmingen, San Diego, CA). From the clear supernatant of the cell lysate obtained by centrifuging at 40,000xg for 45 min, ETK was affinity-purified by the 6xHis purification kits (Cat. No. 21474K, Pharmingen, San Diego, CA) according to the supplier's instruction.

**Autophosphorylation of Recombinant ETK Constructs In Vitro.** GST fusion protein of human ETKC, a constitutively activated ETK mutant (residues 243–674) which lacks the N-terminal PH domain was affinity-purified from bacteria (E. coli). The GST-ETKC (0.6 μg) was incubated in the kinase buffer containing 10 μM ATP (with or without 5 μCi of [γ-$^{32}$P]-ATP) as described previously[8] in the presence or absence of AG879 (10 nM or 1–10 mM) at 37°C for 40 min. The auto-phosphorylation was then monitored by immuno-blotting the protein separated by the SDS-PAGE and transferred onto nitrocellulose with anti-phospho-Tyr antibody (or by radio-autography). Similarly 3 μg of full-length ETK purified from the insect cells was incubated in the buffer containing 30 mM PIPES, pH 7.0, 10 μM $MnCl^2$, 30 μM ATP, 5 μCi of [γ-$^{32}$P] ATP, 1 mM $Na_3VO_4$ for 20 min at 30°C, in the presence or absence of AG879 (10 nM–1 mM), and the auto-phosphorylation was measured by radio-autography of the proteins separated on SDS-PAGE.

**Upregulation of ETK by RAS.** The ETK protein levels were compared between normal NIH/3T3 cells and two distinct v-Ha-RAS transformed cell lines, excluding the possible clonal difference in the ETK levels: stable v-Ha-RAS cell line (RAS cells) and doxycycline-inducible v-Ha-RAS transformants prepared as described previously.[20,21] The lysates of both normal and RAS cells (20 μg protein of each) were subjected to SDS-PAGE and immuno-blotted by the anti-ETK antibody. In the case of doxycycline-inducible RAS transformants, cells were incubated for 2–3 days in the presence or absence of 2 μg/ml doxycycline, and each lysate (20 μg protein) was subjected to the SDS-PAGE/ immuno-blot with the anti-ETK.

## RESULTS

**AG879 (10 nM) Blocks the Activation of PAK1 and Suppresses RAS-Induced Malignant Transformation.** AG879 was reported as an inhibitor specific for both ErbB2 and VEGF receptor FLK-1 (IC50 is around 1 mM)[12,13] and appears to be metabolically more stable than AG825 in vivo as it strongly suppresses the growth of RAS-sarcomas in nude mice.[2] However, the $IC_{50}$ of AG879 for inhibiting PAK1 activation and RAS transformation in vitro still remained to be determined.

10 nM AG879 strongly blocks PAK1 kinase activity in RAS cells without affecting the PAK1 protein level (Fig. 1A). However, AG879 does not inhibit the kinase activity of the purified GST-PAK1 fusion protein directly even at 1 μM (Fig. 1B). These observations suggest that ErbB2 is not involved in the inactivation by AG879 of PAK1 in cells. Interestingly, AG879 also suppresses the anchorage-independent growth of RAS cells in soft agar (Fig. 1C). The $IC_{50}$ of AG879 for the large colony formation is 1–10 nM. However, the inhibition of anchorage-independent growth by AG879 is not due to non-specific inhibition on cell growth, as at even 100

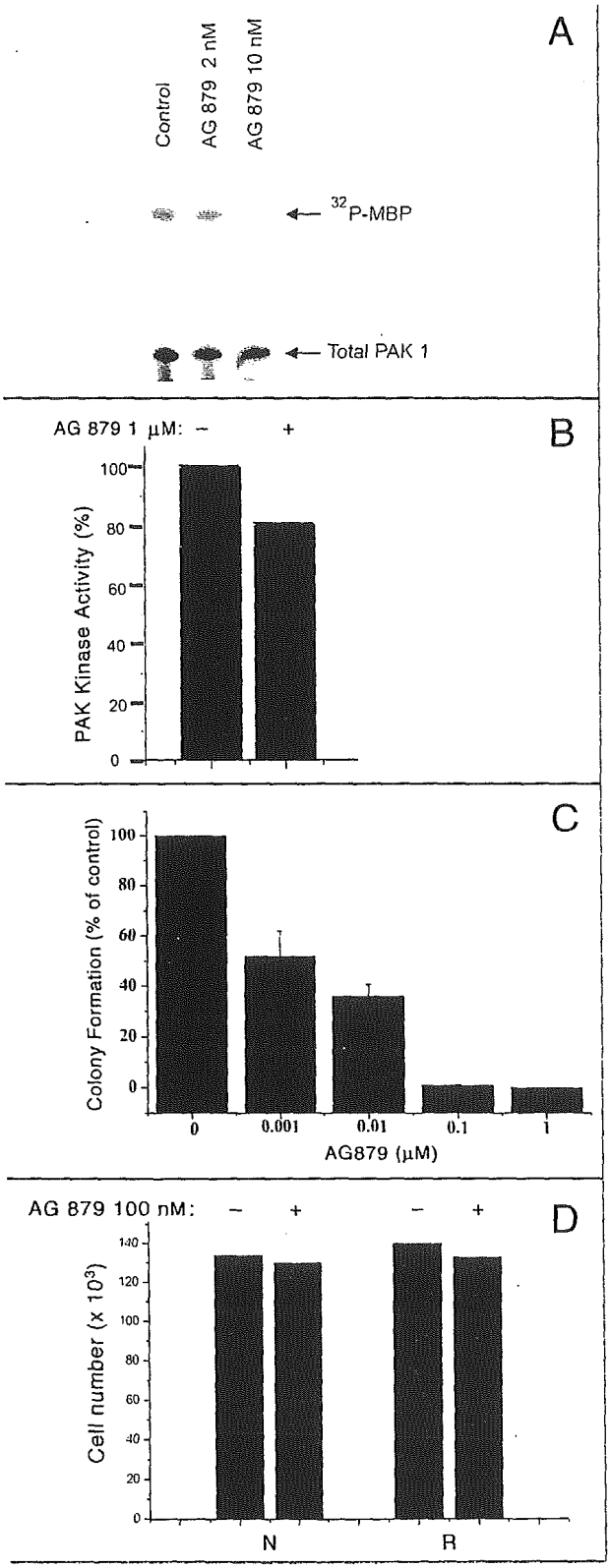


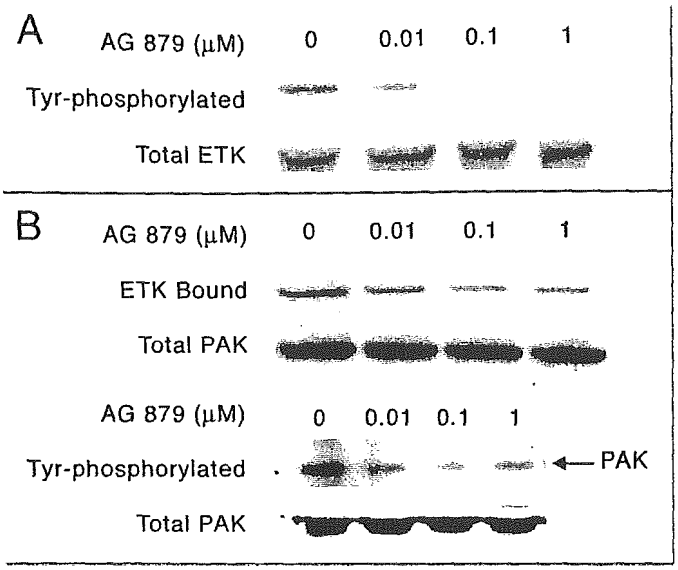


Figure 2. AG879 blocks the Tyr-phosphorylation of ETK and its association with PAK1. (A) Serum-starved RAS cells were first incubated with AG879 (0.01-1 μM) for 1hr. The cells lysates (CL) were then immuno-precipitated (IP) with the anti-ETK antibody as described under "Materials & Methods", followed by immuno-blot (IB) with anti-phospho-Tyr (PY) antibody. (B) Alternatively, the CL were IP with the anti-PAK1 (top panel) or anti-PY (bottom panel) antibodies, followed by IB with anti-ETK (top panel) or anti-PAK1 (bottom panel) antibodies. The total PAK1 protein level of the bottom panel was determined by IBing each CL directly. Similar results were obtained from two or three independent experiments.

nM AG879 does not affect the anchorage-dependent growth of either normal or RAS-transformed NIH 3T3 cells (Fig. 1D). These results suggest that the suppression by AG 879 of both RAS-induced malignant transformation and PAK1 activation is not due to blocking ErbB2, but another kinase(s) associated with PAK1.

**AG879 Inhibits the Tyr-Phosphorylation of ETK and Its Association with PAK1.** The Tyr-phosphorylation of PAK1 is required for its Ser/Thr kinase activity as the treatment of PAK1with a Tyr-phosphatase reduces its kinase activity.[22] Activated ETK associates with PAK1 through its PH domain and activates PAK1 by the Tyr phosphorylation.[11] To test whether the Tyr kinase activity of ETK is affected by AG879, serum-starved RAS cells were treated with AG879 (0.01–1 μM) in culture for 1hr. Cell lysates were then immuno-precipitated with the anti-ETK antibody, followed by immuno-blotting with the anti-phospho-Tyr or anti-ETK antibody. AG879 inhibits the Tyr-phosphorylation of ETK at 10 nM, but does not affect the ETK protein level (Fig. 2A). Furthermore, using the anti-PAK1 antibody, we found that AG879 significantly suppresses the ETK-PAK1 association (Fig.2B, top panel) and reduced the Tyr-phosphorylation of PAK1 in cells at 10 nM (Fig.2B, bottom panel). These results suggest that AG879 inhibits somehow the kinase activity of ETK, thus blocking its auto-phosphorylation, and association with PAK1, and the Tyr-phosphorylation of PAK1 by ETK.

**AG879 Inactivates ETK In Vitro.** To determine whether AG879 directly inhibits the kinase activity of ETK or not, RAS cells were lysed and

Figure 1. (A) AG879 inhibits the activation of PAK1 in cells. Serum-starved RAS cells were incubated with AG879 (0.01–10 μM) for 1hr. The cell lysates were subjected to PAK kinase assay as described under "Materials & Methods". 10 nM AG 879 clearly inhibited the PAK1 activity (phosphorylation of MBP) in cells (top panel). Similar levels of PAK1 protein were detected in all lanes as judged by immuno-blot (bottom panel). (B) PAK1 is not a direct target of AG 879. 1 μM AG 879 fails to inhibit significantly the kinase activity of GST-PAK1 in vitro. (C) AG879 inhibits anchorage-independent growth of RAS cells. RAS cells were planted in soft agar with or without AG879 (0.001–100 μM) as described under "Materials & Methods". The colony formation was measured in comparison with that of the control (non-treated) cells. Only large colonies consisting more than 100 cells per colony were counted. The presented values are the average of those obtained from two independent experiments. (D) AG 879 has no effect on the anchorage-dependent cell growth. The growth of either normal or RAS-transformed cells in liquid culture was monitored in the presence or absence of 100 nM AG 879 as described under "Materials & Methods".

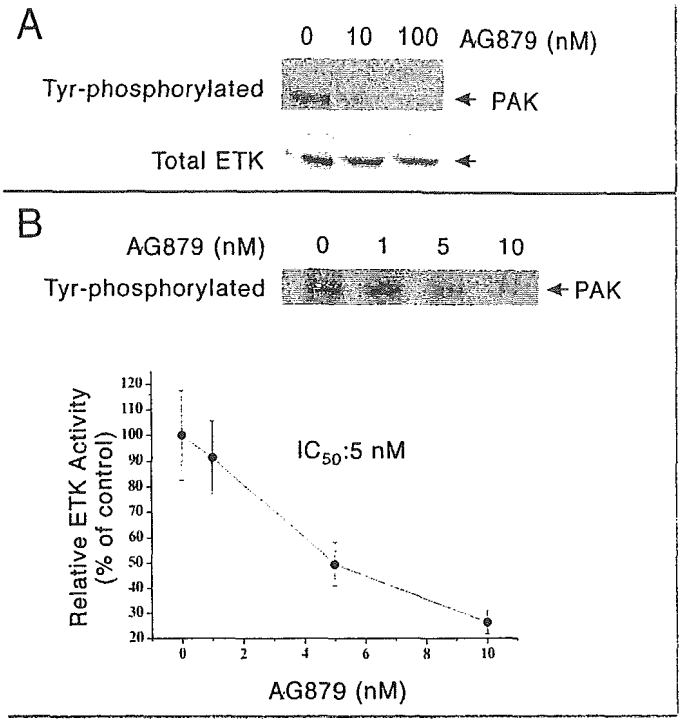


Figure 3. AG879 inhibits the kinase activity of ETK in vitro. The lysates of RAS cells were immuno-precipitated by anti-ETK antibody. The immuno-precipitates (IB) were subjected to an in vitro kinase assay in the presence or absence of AG879 (A, 10 or 100 nM; B, 1 to 10 nM) as described under "Materials & Methods". The ETK activity (Tyr-phosphorylation of PAK1) was monitored by immuno-blot (IB) with anti-PY antibody. Similar protein levels of ETK were detected in all lanes by IB with the anti-ETK antibody. Similar results were obtained from two independent experiments.

immuno-precipitated with the anti-ETK antibody. The immuno-precipitates were subjected to an in vitro kinase assay in the presence or absence of AG879 (0.001–10 μM) as described in the "Materials and Methods". AG879 (10 nM) strongly inhibits the Tyr-phosphorylation of PAK1 by

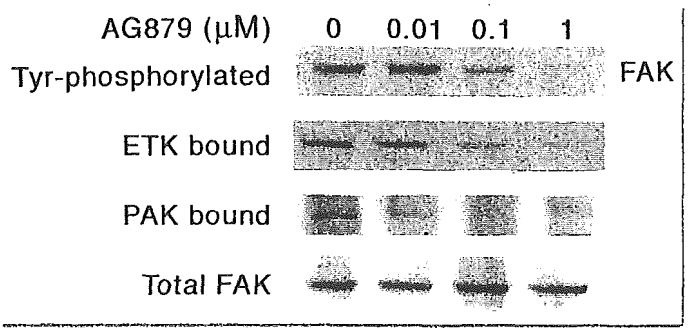


Figure 5. AG879 suppresses the Tyr-phosphorylation of FAK and its association with ETK and PAK1. Serum-starved RAS cells were incubated with AG879 (0.01–1 μM) for 1hr. The cell lysates were immuno-precipitated (IP) with anti-FAK antibody as described under "Materials & Methods", followed by immuno-blot (IB) with anti-phospho-Tyr (PY), anti-ETK or anti-PAK antibodies. Similar protein levels were detected in all lanes by IB with the anti-FAK antibody. Similar results were obtained from two independent experiments.

ETK (Fig.3A), and the $IC_{50}$ for ETK is around 5 nM (Fig. 3B). Furthermore, AG 879 has no direct effect on any other members of TEC family kinases such as TEC, BTK or ITK, even at 10 μM in vitro (data not shown). These results suggest that ETK is so far most sensitive to the action of AG879. However, since the anti-ETK antibody could precipitates not only ETK itself, but also any proteins forming a tight complex with ETK such as PAK1 and FAK, we cannot exclude the possibility that the primary target of AG 879 might be a third Tyr-kinase which is associated with ETK, and responsible for the ETK activation.

**AG879 (5 nM) Does Not Inhibit Recombinant ETK from Bacteria or Insect Cells.** To clarify whether ETK itself is the primary target of ETK, two different recombinant ETK samples of human origin were purified from bacteria or insect cells: a constitutively activated mutant of ETK called ETKC (residues 243–674) which lacks the N-terminal PH domain purified from bacteria as a GST fusion protein, and full-length ETK purified from insect cells. Either the ETKC or the full-length ETK were not inhibited by AG 879 at 10 nM, although they were significantly inhibited at 1–10 μM (see Fig. 4). Furthermore, in vitro binding of PAK1 in RAS cell lysates to either the PH domain of ETK or a kinase-dead mutant of ETK (called

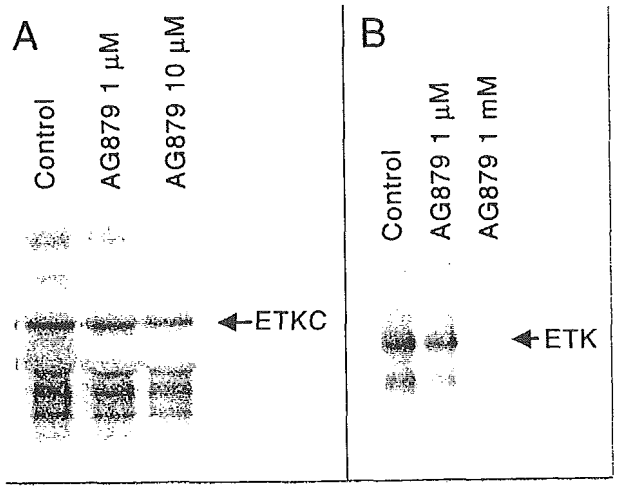


Figure 4. Recombinant ETK proteins alone are far less sensitive to AG 879 in vitro. (A) Effect of AG879 on the ETKC from bacteria. The GST-ETKC was auto-phosphorylated in the presence of AG 879 (0, 1 and 10 μM) in vitro as described under "Materials and Methods". (B) Effect of AG879 on full-length ETK from insect cells. The full-length ETK was auto-phosphorylated in the presence of AG 879 (0, 1 μM and 1mM) in vitro as described under "Materials and Methods".

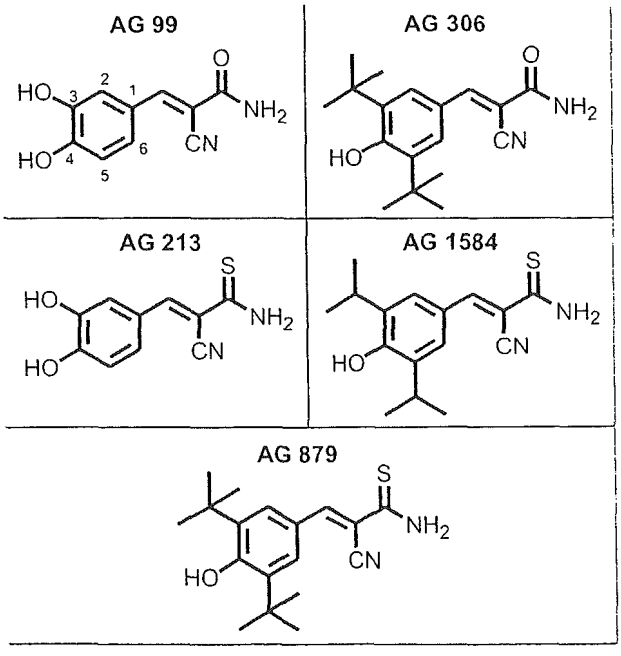


Figure 6. Chemical structure of AG 879 derivatives.

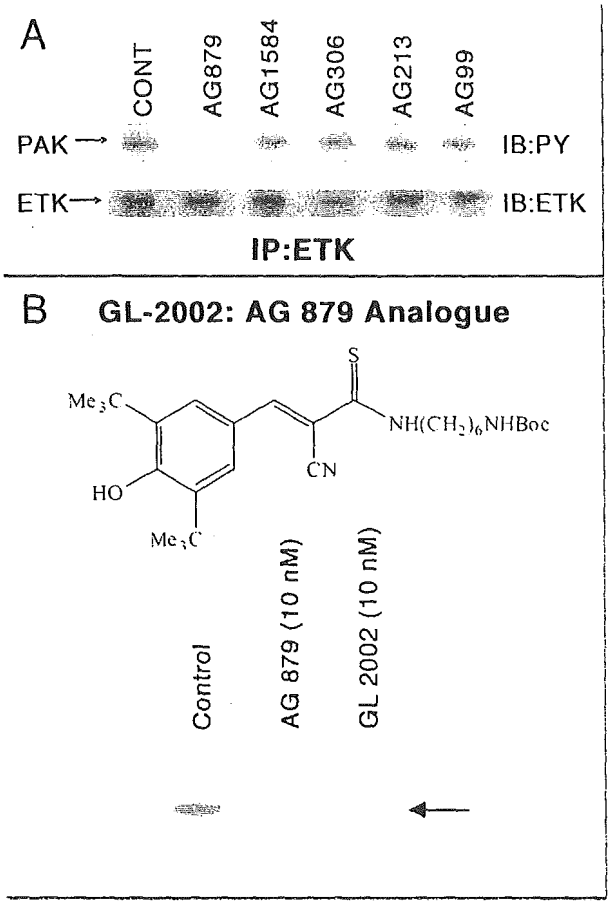


Figure 7. Anti-ETK activity of AG 879 derivatives. (A) The lysates of RAS cells were immuno-precipitated by anti-ETK antibody. The immuno-precipitates (IP) were subjected to an in vitro kinase assay in the absence of any drug (CONT) or presence of either AG879 (10 nM) or four other derivatives (10 μM) as described in Figure 3. Only AG 879 inhibits the ETK activity (Tyr-phosphorylation of PAK1) monitored by immuno-blot (IB) with anti-PY antibody. Similar protein levels of ETK were detected in all lanes by IB with the anti-ETK antibody. Similar results were obtained from two independent experiments. (B) After RAS cells were treated with either 10 nM GL-2002 or AG 879 for 1.5 hrs, each cell lysate was subjected to the in vitro PAK1 kinase assay described in Fig. 1B. GL-2002 strongly inhibited PAK1 activation as did AG 879. Similar results were obtained from three independent experiments.

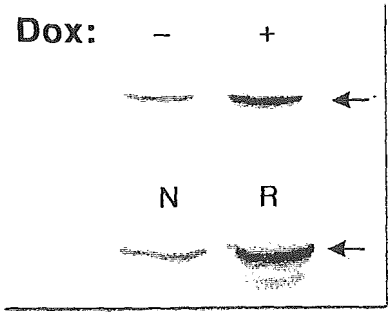


Figure 8. RAS-induced up-regulation of ETK. Upper panel: Up-regulation of ETK by the Doxycyline-induced v-Ha-RAS expression in normal NIH/3T3 cells. Dox-minus, the control (no doxycycline-added); Dox-plus, 2 μg/ml doxycycline added. Lower panel: Enhanced expression of ETK in v-Ha-RAS-transformants. N, normal NIH/3T3 cells; R, v-Ha-RAS-transformants. The arrow indicates the ETK band. Both stable and inducible RAS up-regulate the ETK protein level.

ETK/KQ) as a GST-fusion protein was not inhibited by 10 nM AG879 (Hirokawa Y, He H, Maruta H, unpublished observation, 2002). These observations altogether suggest that the primary target of AG879 is not ETK itself, but rather its associated upstream activator to be identified.

**AG879 Inhibits the Tyr-Phosphorylation of FAK and Its Association with ETK and PAK1.** ETK is a cytoplasmic (non-receptor) Tyr kinase which is activated at the plasma membranes.[9,10] The N-terminus of FAK shares significant sequence homology with FERM domains, which are involved in linking cytoplasmic proteins to the membranes.[23,24] It was shown recently that the activation of ETK by extracellular matrix (ECM) is regulated by FAK through the interaction between the PH domain of ETK and the FERM domain of FAK, and that activated FAK binds ETK and elevates the Tyr-phosphorylation of ETK.[8]

To test whether the FAK-ETK interaction is affected by AG879, serum-starved RAS cells were treated with AG879 (0.01–1μM). Cell lysates were then immuno-precipitated with anti-FAK antibody, followed by blotting with anti-phospho-Tyr, anti-ETK or anti-PAK1 antibodies separately. As shown in Figure 5, AG879 suppresses both the Tyr-phosphorylation of FAK and its association with ETK at 100 nM, but not at 10 nM, whereas AG879 inhibits the FAK-PAK1 interaction at 10 nM. These results suggest that PAK1 associates with FAK probably through ETK, and PAK1 can no longer interact with FAK when the PAK1-ETK complex is disrupted by AG879.

**The Structure-Function Analysis of AG879 Derivatives in Inhibiting ETK.** To determine which side chains of AG879 are essential for the ETK inhibition, and further screen for a more potent "ETK inhibitor", we have examined the anti-ETK activity of several AG879 derivatives shown in Figure 6. However, none of these derivatives other than AG879 itself inhibits ETK activity in vitro even at 10 μM (see Fig. 7A). These results indicate that at least both tert butyl groups at positions 3 and 5, and the thio group are absolutely essential for AG879 to inhibit ETK. Interestingly, the ErbB2-specific inhibitor AG825 is distantly related to AG879, but like AG306, lacks both the thio and tert butyl groups, and in fact shows no anti-ETK activity at even 1 μM in vitro (data not shown). However, when the free (thio) amino group of AG879 was alkylated with an amino-hexane chain, the resulting derivative called GL-2002 was still able to show a strong anti-ETK activity that blocks the PAK1 activation in RAS cells even at 10 nM (Fig. 7B), suggesting that, unlike other side chains, this free amino group of AG879 is not essential for its anti-ETK activity. Thus, we are currently generating a series of bioactive immobilized AG 879 (or its water-soluble N-hexylamine derivative, called GL-2003) by coupling them to agarose beads through the amino group so that we can use the AG879/GL-2003 bead as a ligand for fishing a high-affinity AG879-binding protein(s).

**Upregulation of ETK Protein Level by RAS.** How does RAS activate this integrin/FAK/ETK pathway? Although the whole picture of this mechanism still remains to be unveiled , we found that v-Ha-RAS upregulates the protein level of ETK several folds, using both doxycycline-inducible v-Ha-RAS transformants and stable v-Ha-RAS transformants derived from normal NIH/3T3 cells (see Fig. 8), clearly indicating that oncogenic RAS signalling involves ETK.

## DISCUSSION

In this study, we have demonstrated that AG879 selectively inactivates the cytoplasmic Tyr kinase ETK with $IC_{50}$ of about 5 nM. The inactivation of ETK by AG879 blocks the ETK-PAK1 interaction, thereby blocking the Tyr-phosphorylation of PAK1 and its kinase activity. Interestingly at this concentration AG879 does not inhibit directly any other kinases including FAK, PAK, ErbB2, ErbB1, TRK, TEC, BTK and ITK. However, since the $IC_{50}$ of this drug for recombinant ETK proteins alone is 1–10 μM, instead of 5 nM, it is most likely that the primary target of AG879 is not ETK, FAK or ErbB2 themselves, but an as yet unidentified activator of ETK. Thus, we are currently identifying this highly AG879-sensitive

target among the kinases which are associated with ETK, Tyr-phosphorylate the kinase-dead (non-auto-phosphorylatable) mutant of ETK (ETK-KQ), and bind tightly to the AG879/GL-2003 beads. Our preliminary data suggest that the primary target is a Tyr-phosphorylated protein of 62 kDa (Hirokawa Y and Maruta H, unpublished observation).

ETK is required for the anchorage-independent and tumorigenic growth of human breast cancer cells.[11] Although ETK alone is not transforming, it enhances malignant transformation of NIH 3T3 cells caused by a partially activated c-Src mutant.[25] ETK can also be activated by Src family kinases and is responsible for Src activation of signal transducer and activator of transcription factor 3 (STAT3) and v-Src-induced transformation.[25] In this study we have established that ETK is essential for RAS transformation: the concentration of AG879 that inhibits both RAS-induced PAK1 activation and anchorage-independent growth is similar to the $IC_{50}$ for ETK both in vitro and in vivo.

We have established here that RAS signalling involves ETK by demonstrating that RAS significantly up-regulates the ETK protein level. To understand further the detailed mechanism, we are currently investigating whether this regulation is at either transcriptional or translational levels or its stability (turn-over rate). In this context, it is worth noting that ETK is highly expressed in metastatic prostate and breast carcinoma cell lines such as PC3M which carry oncogenic Ki-RAS mutants.[8] Since RAS cells in general are both metastatic and angiogenic, it is conceivable that at least a part of the reason for the high expression of ETK in these cell lines might be due to the constitutive RAS activation. Thus, it would be of great interest to determine whether AG879 inhibits the metastasis of these RAS cancer cell lines in vivo.

It was suggested earlier that AG879 (also called SU0879) suppresses angiogenesis by blocking VEGF receptor FLK-1.[13] However, since the VEGF receptor also directly activates ETK[10] which is then inhibited by AG879 at 5 nM (200 times more sensitive to this drug than FLK-1), it is more likely that AG879 suppresses angiogenesis primarily by blocking ETK, rather than FLK-1. Since oncogenic RAS mutants up-regulate expression of VEGF through Raf-MEK-MAP kinase cascade,[26] and VEGF in turn activates ETK through FLK-1in endothelial cells, RAS transformation can induce angiogenesis through this paracrine pathway. Thus, it is conceivable that the suppression of RAS sarcomas growth by AG879 in mice[2] might be at least in part due to its anti-angiogenic action, (in addition to blocking the anchorage-independent growth of RAS cells per se). Interestingly it was recently shown that PAK1 is essential for angiogenesis. A cell-permeable peptide which blocks selectively the NCK-PAK1 interaction inhibits bFGF-induced angiogenesis.[27]

## References


1. Tang Y, Chen Z, Ambrose D, Liu J, Gibbs JB, Chernoff J, Field J. Kinase-deficient Pak1 mutants inhibit Ras transformation of Rat-1 fibroblasts. Mol Cell Biol 1997; 17:4454-64.
2. He H, Hirokawa Y, Manser E, Lim L, Levitzki A, Maruta H. Signal therapy for RAS-induced cancers in combination of AG 879 and PP1, specific inhibitors for ErbB2 and Src family kinases, that block PAK activation. Cancer J 2001 7:191-202.
3. Manser E., Loo TH, Koh CG, et al. PAK kinases are directly coupled to the PIX family of nucleotide exchange factors. Mol Cell 1998; 1:183-92.
4. Bagrodia S, Bailey, D, Lenard, Z, et al. A tyrosine-phosphorylated protein that binds to an important regulatory region on the cool family of p21-activated kinase-binding proteins. J Biol Chem. 1999; 274:22393-400.
5. Galisteo M, Chenoff J, Su YC, et al. The adaptor protein Nck links receptor tyrosine kinases with the serine-threonine kinase Pak1. J Biol Chem 1996; 271:20997-1000.
6. He H, Hirokawa Y, Levitzki A, Maruta H. An anti-Ras cancer potential of PP1, an inhibitor specific for Src family kinases: in vitro and in vivo studies. Cancer J 2000; 6:243-8.
7. Lambert J, Lambert Q, Reuther G, Malliri A, Siderovski D, Sondek J, et al. Tiam1 mediates RAS activation of Rac by a PI-3 kinase-independent mechanism. Nat Cell Biol 2002; 4:621-5.
8. Chen R, Kim O, Li M, Xiong X, Guan JL, Kung HJ, et al. Regulation of the PH-domain-containing tyrosine kinase Etk by focal adhesion kinase through the FERM domain. Nat Cell Biol 2001; 3:439-44.
9. Qiu Y, Kung HJ. Signaling network of the Btk family kinases. Oncogene 2000; 19:5651-61.
10. Smith CI, Islam TC, Mattsson PT, Mohamed AJ, Nore BF, Vihinen M. The Tec family of cytoplasmic tyrosine kinases: mammalian Btk, Bmx, Itk, Tec, Txk and homologs in other species. Bioessays 2001; 23:436-46.
11. Bagheri-Yarmand R, Mandal M, Taludker AH, Wang RA, Vadlamudi RK, Kung HJ, Kumar R. Etk/Bmx tyrosine kinase activates Pak1 and regulates tumorigenicity of breast cancer cells. J Biol Chem 2001; 276:29403-9.
12. Levitzki A, Gazit A. Tyrosine kinase inhibition: an approach to drug development. Science 1995; 267:1782-8.
13. Strawn L, McMahon G, App H, Schreck R, et al. Flk-1 as a target for tumor growth inhibition. Cancer Res 1996; 56:3540-5.
14. Qiu Y, Robinson D, Pretlow T, Kung HJ. Etk/Bmx, a tyrosine kinase with a pleckstrin-homology domain, is an effector of phosphatidylinositol 3'-kinase and is involved in interleukin 6-induced neuroendocrine differentiation of prostate cancer cells. Proc Natl Acad Sci USA 1998; 95:3644-9.
15. Maruta H, Holden J, Sizeland A. D'Abaco G. The residues of Ras and Rap proteins that determine their GAP specificities. J Biol Chem 1991; 266:11661-8.
16. Obermeier A, Ahmed S, Manser E, Yen SC, Hall C, Lim L. PAK promotes morphological changes by acting upstream of Rac. EMBO J 1998; 17:4328-39.
17. Nheu T, He H, Hirokawa Y, Tamaki K, et al. The K252a derivatives, inhibitors for the PAK/MLK kinase family, selectively block the growth of RAS transformants. Cancer J 2002; 8:328-35.
18. Bellis SL, Miller JT, Turner CE. Characterization of tyrosine phosphorylation of paxillin in vitro by focal adhesion kinase. J Biol Chem 1995; 270:17437-41.
19. He H, Levitzki A, Zhu HJ, Walker F, Burgess A, Maruta H. Platelet-derived growth factor requires epidermal growth factor receptor to activate p21-activated kinase family kinases. J Biol Chem 2001; 276: 26741-4.
20. Zhu HJ, Iaria J, Sizeland A. Smad7 differentially regulates TGF-β-mediated signalling pathways. J Biol Chem 1999; 274:32258-64.
21. Zhu HJ, Nheu T, Cheng HC, Iaria J, Simpson R, Maruta H, Burgess AW. Oncogenic RAS transformation downregulates the expression of the PTEN tumor suppressor. Cancer Res 2003; In press.
22. McManus MJ, Boerner JL, Danielsen AJ, Wang Z, Matsumura F, Maihle NJ. An oncogenic epidermal growth factor receptor signals via a p21-activated kinase-caldesmon-myosin phosphotyrosine complex. J Biol Chem 2000; 275:35328-34.
23. Chishti AH, Kim AC, Marfatia SM, et al. The FERM domain: a unique module involved in the linkage of cytoplasmic proteins to the membrane. Trends Biochem Sci 1998; 23:281-2.
24. Girault JA, Labesse G, Mornon JP, Callebaut I. The N-termini of FAK and JAKs contain divergent band 4.1 domains. Trends Biochem Sci 1999; 24:54-7.
25. Tsai YT, Su YH, Fang SS, Huang TN, Qiu Y, Jou YS, Shih HM, Kung HJ, Chen RH. Etk, a Btk family tyrosine kinase, mediates cellular transformation by linking Src to STAT3 activation. Mol Cell Biol 2000; 20:2043-54.
26. Grugel S, Finkenzeller G, Weindel K, et al. Both v-Ha-Ras and v-Raf stimulate expression of the vascular endothelial growth factor in NIH 3T3 cells. J Biol Chem. 1995;270:25915-9.
27. Kiosses W, Hood J, Yang S, et al. A dominant-negative PAK peptide inhibits angiogenesis. Circ Res 2002; 90:697-702.

# Genistein-Induced Changes in Gene Expression in Panc 1 Cells at Physiological Concentrations of Genistein

*Jianfeng Bai, MD,*† Naohiro Sata, MD, PhD,* Hideo Nagai, MD, PhD,* Tomoaki Wada, MD, PhD,‡ Koji Yoshida, MD, PhD,§ Hiroyuki Mano, MD, PhD,§ Fumihiro Sata, MD, PhD,‖ and Reiko Kishi, MD, PhD‖*

**Objectives:** To investigate the effect of genistein on gene expression in Panc 1 cells using microarray technology.

**Methods:** Panc 1 cells were treated with 10 μmol/L genistein or DMSO (vehicle control) for 0, 1, 3, 6, or 12 hours. Total RNA from each sample was isolated, and biotin-labeled probes were hybridized to the human genome U133A chip, after which the chip was washed and scanned. Data were analyzed using DMT software (Affymetrix). For genes that showed large changes in expression due to genistein, these changes were confirmed using real-time PCR assays.

**Results:** Two independent microarray experiments showed that genistein significantly changed the expression of 47 genes: up-regulating of egr-1 and IL-8 and down-regulating of EGF-R AKT2, CYP1B1, NELL2, SCD, DNA ligase III, Rad as well as 18s and 28s rRNA and others. These alterations in expression were confirmed using real-time PCR, although the increase in change was not exactly the same in the 2 assays.

**Conclusions:** Our data suggest the reported apparent ability of genistein to inhibit carcinogenesis may involve a number of pathways. The most obvious target is the EGF-R signaling pathway since the expression of 5 genes related to this pathway was reduced (EGFR, egr-1, AKT2, CYP1B1, and NELL2). Genistein may also act by disabling cancer cell self-protection by inhibiting expression of AKT2, CYP1B1, and DNA ligase III. Furthermore, genistein may inhibit carcinogenesis by inhibiting expression of SCD. Finally, our data support findings indicating that genistein inhibits rRNA formation, which is an important mechanism by which genistein regulates tumor cell growth.

Received for publication August 26, 2003; accepted February 2, 2004.

From the *Department of Surgery, Jichi Medical School, Tochigi, Japan; †Department of Surgery, The First Affiliated Hospital of Nanjing Medical University, Nanjing, China; ‡Department of Gynecology, Jichi Medical School, Tochigi, Japan; §Division of Functional Genomics, Jichi Medical School, Tochigi, Japan; and ‖Department of Public Health, University of Hokkaido, Hokkaido, Japan.

This study was supported by Grants-in-Aid for Scientific Research of the Japanese Society of the Promotion of Science.

Reprints: Naohiro Sata, MD, PhD, Department of Surgery, Jichi Medical School, 3311-1 Yakushiji, Minamikawachi, Tochigi 329-0498, Japan (e-mail: sata@jichi.ac.jp).



**Key Words:** genistein, physiological concentration, Panc 1, microarray

(*Pancreas* 2004;29:93–98)

Genistein, a component of soybeans, has received much attention because of its possible health benefits. Epidemiological reports and laboratory data have associated genistein with reduced incidence of endometrial, breast, prostate, and pancreatic cancers; cardiovascular disease and osteoporosis; and lower total blood cholesterol.[1] Genistein has been reported as a clinically effective and well-tolerated anticancer drug in advanced cases of chemotherapy-resistant acute childhood lymphoblastic leukemia as well as adult chronic lymphocytic leukemia.[2] Genistein has previously been reported as an antagonist of estrogen receptors and shown to inhibit the activity of protein tyrosine kinases, DNA topoisomerase II, and tyrosine autophosphorylation of epidermal growth factor, and expression of transforming growth factor β, somatostatin in vitro.[3–6] Furthermore, genistein can regulate cell cycle progression and cause $G_2$-M arrest.[7] Genistein also inhibits nucleic acid ribose synthesis through the nonoxidative reactions of the pentose cycle.[8] However, most of these activities have been observed only at genistein concentrations in excess of those attainable physiologically in humans, eg, 18.5 μmol/L or 5 μg/mL.[9]

While a number of reports are consistent with the possible anticancer effects of genistein, there are reports suggesting the contrary. Ju et al[10] showed that physiological concentrations of dietary genistein enhanced the growth of implanted tumors because of its estrogenic effect. Others report that dietary genistein negated the inhibitory effect of tamoxifen on the growth of estrogen-dependent human breast cancer (MCF) cells implanted in athymic mice.[11] The reasons for the different activities of genistein remain to be ascertained.

If genistein contained in soybeans does contribute to a lower incidence of some diseases in Asian populations, this would reflect its effect at physiological concentrations. In the present study, we used microarray technology to examine the effects of a physiological concentration of genistein (10 μmol/L) on gene expression in Panc1 cells.

## MATERIALS AND METHODS

### Cell Culture and Growth Inhibition

Panc 1 cell lines were cultured in D-MEM/F-12 media (GIBCO, Life Technologies, Tokyo, Japan) supplemented with 10% fetal bovine serum (GIBCO) and 1% penicillin and streptomycin (GIBCO) in a 5% $CO_2$ atmosphere at 37°C. Genistein (Sigma-Aldrich, Tokyo, Japan) was dissolved in DMSO to make a 10 mmol/L stock solution for experiments. To examine the effect of genistein concentration on proliferation, $1 \times 10^5$ Panc 1 cells were plated in 10-cm dishes and 24 hours later treated with 10, 20, 50, 100, and 200 μmol/L genistein or DMSO (vehicle control) for a further 1 to 4 days. Cell survival was determined by counting cell numbers in a counting chamber. Each sample had 3 replicates, and each experiment was performed 3 times.

### Oligomicroarray Analysis of Gene Expression Profiles

Panc 1 cells were treated with 10 μmol/L genistein or DMSO for 0, 1, 3, 6, or 12 hours. Purified total RNA from each sample was isolated using the RNeasy Mini Kit (QIAGEN, Tokyo, Japan) and the RNase-free DNase Set (QIAGEN), according to the manufacturer's protocols. cDNA was synthesized using the Superscript cDNA Synthesis Kit (Invitrogen Japan, Nihonbashi, Japan), using T7-dT primer in place of the oligo(dT) provided in the kit, and this double-stranded cDNA was purified using the QIAquick PCR Purification Kit (QIAGEN). Using this cDNA, biotin-labeled cRNA was transcribed using the ENZO BioArray Labeling Kit (Affymetrix, Los Angeles, CA) and purified using the RNeasy Mini Kit. The cRNA was fragmented in 5′ fragmentation buffer at 94°C for 35 minutes and chilled on ice. The fragmented biotin-labeled cRNA was hybridized to the human genome U133A chip (Affymetrix) in a Genechip 640 hybridization oven (Affymetrix) for 16 hours. Washing and staining of the chip were done in a Genechip Fluidics Station 400 (Affymetrix). Finally, the chip was scanned using an Affymetrix array scanner. This procedure was performed twice.

### Microarray Data Normalization and Analysis

The signals of samples were normalized and analyzed using Microarray Suite and Data Mining Tool software (Affymetrix). Genes whose signal values were less than 15 at all five time points were considered as not or poorly expressed in Panc 1 cell lines and were not involved in further analysis. The value of 15 was decided on as a result of our experience with this system. Results were exported as .txt files. Complete-linkage hierarchical clustering and display of the exported data were applied using the free downloadable software Cluster and TreeView (Michael Eisen http://rana.lbl.gov/EisenSoftware.htm).

### Verification by Real-Time PCR

Total RNA used for microarray was also used for real-time PCR analysis. First, primers were designed for the genes of interest using GENETYX software. Then, PCR conditions were optimized for each pair of primers (QuantiTec SYBR Green PCR Kit; QIAGEN). After that, first strand cDNA was synthesized from 2 μg total RNA (Superscript First Strand cDNA Synthesis Kit), and 1 μL RT-PCR product was used in real-time PCR under the optimized reaction conditions. The components of the 50 μL reaction mixture were 25 μL SYBR Green PCR Master Mix, 1 μL sense primer, 1 μL antisense primer, 1 μL cDNA, 0.5 μL uracil-*N*-glycosylase, and 21.5 μL RNase-free water. The real-time cycler conditions were 50°C (2 minutes) → 95°C (10 minutes) → [94°C (15 seconds) → optimized annealing temperature (30 seconds) → 72°C (30 seconds), 50 cycles]. β-actin was used as control to normalize the amount of cDNA used. After the reaction, products were analyzed using 2% agarose gel electrophoresis to confirm that the signals detected by the GeneAmp PCR system 7700 were from the expected products. Three independent experiments were performed. Sequences of some primers are listed in Table 1.

## RESULTS

### Genistein Inhibition of Panc 1 Cell Proliferation

We compared surviving cells observed in control vehicle–treated cultures of Panc 1 cells with those in cultures

**TABLE 1.** Sequences of Primers for Checked Genes

| Gene | Sense | Antisense |
|---|---|---|
| β-actin | AATCTGGCACCACACCTTCTAC | GCTTCTCCTTAATGTCACGCAC |
| egr-1 | CAGTGGCCTAGTGAGCATGA | AGTAGACAGAGGGGTTAGCGA |
| AKT2 | CCATGAATGAGGTGTCTGTC | ACGGAGAAGTTGTTTAAGGG |
| EGFR | TGCGGTTCAGCAACAACCCT | GCTGGGCACAGATGATTTTGGTC |
| CYP1B1 | TCTTGCCCTAGGCAAAGGTC | GATAGTGGCCGGTACGTTCT |
| NELL2 | AGAGGGAGACGATGGACTGA | TGATGGCTAAGGAGAGCTTGT |
| Ligase III | ATGGCTGAGCAACGGTTCTG | GCCAGTGGTTGTCAACTTAGCC |

treated with increasing doses of genistein. Cell counting showed that genistein inhibited cell proliferation at concentrations equal to and greater than 20 μmol/L (Fig. 1).

## Genistein Alters Panc 1 Gene Expression

The proliferation studies indicated there was no effect of genistein below 20 μmol/L. Despite this, we examined the effect of 10 μmol/L genistein on gene expression as we believe this concentration is closer to physiological values. Total RNA was extracted from 10 μmol/L genistein-treated and vehicle-treated $1 \times 10^7$ Panc 1 cells, respectively, followed by cDNA synthesis, labeling, hybridization, and scanning. Two independent experiments showed that 47 points met the filter criteria described in the Materials and Methods section (Fig. 2). In this human genome U133 chip analysis, 1 gene was represented by several oligo segments, indicating some of the 47 points referred the same gene. The cluster map of these points clearly showed that all repeated points referring to the same gene were clustered together. The microarray analysis indicated changes in expression of the following genes: up-regulation of egr-1 (early growth response 1) and IL-8 (interleukin-8); down-regulation of EGF-R (epidermal growth factor receptor), AKT2 (v-akt murine thymoma viral oncogene homolog 2), CYP1B1 (cytochrome P450, family 1, subfamily B, polypeptide 1), NELL2 (nel chicken-like 2), SCD (stearoyl-CoA de-

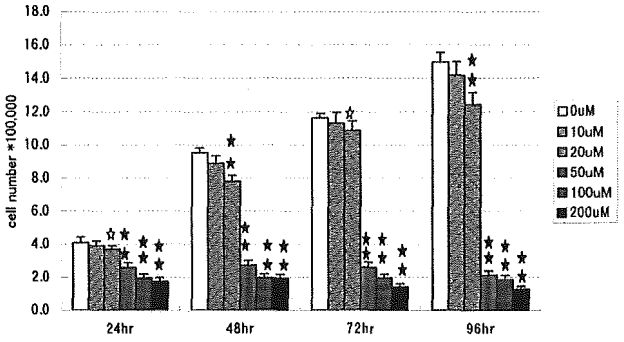


**FIGURE 1.** The growth inhibition curves for Panc 1 cells by genistein: $1 \times 10^5$ Panc 1 cells were maintained in 10-cm culture dishes for 24 hours, followed by the addition of genistein (in DMSO) to the supernatants of the culture cells to the concentrations indicated. The cells were treated for another 1 to 4 days and then subjected to cell proliferation analysis. The number of surviving cells in each experimental condition was expressed as mean ± SEM of 3 independent experiments with 3 repeats. It showed that the proliferation of Panc 1 cells is significantly inhibited by genistein at the concentration of 20 μmol/L and higher compared with DMSO (vehicle)-treated cells (☆$P < 0.05$, ★★$P < 0.01$). Panc 1 cells still retain a rather rapid proliferation rate at 20 μmol/L, while 50 μmol/L and higher concentrations keep the Panc 1 cells at low levels even after 4 days culture. Genistein (10 μmol/L) does not inhibit Panc 1 cell proliferation significantly at any time point.

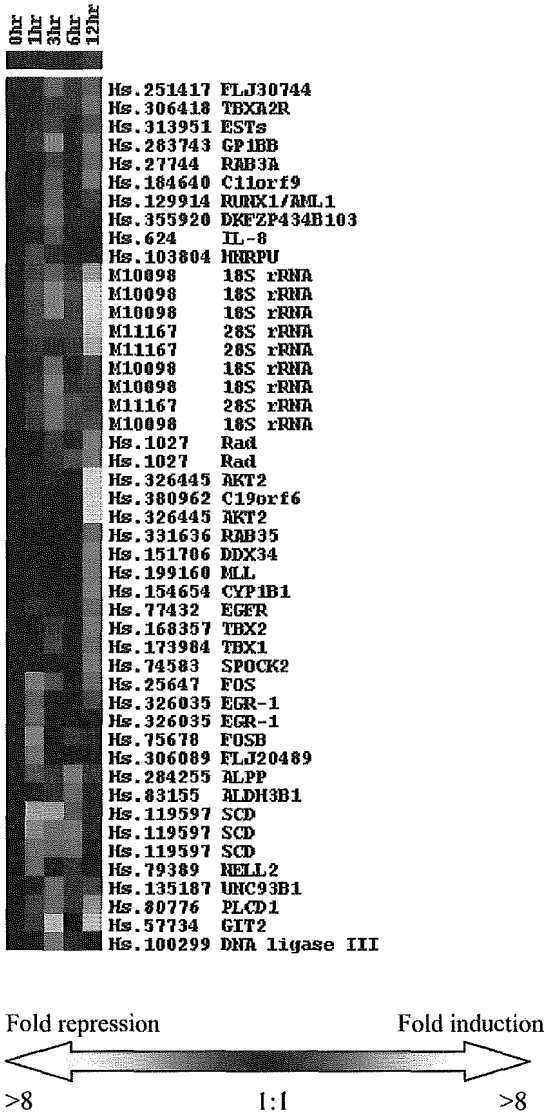


**FIGURE 2.** Cluster map of 47 points that passed the filter criteria described in Materials and Methods. These genes, with their symbols and identification numbers, are listed on the side of their expression profiles that are presented by different intensities of black and white colors. The bar indicator showing lighter color represents the greater folds of induction or repression (up to eight-fold), respectively, as compared to time 0, whereas the unchanged gene expression levels (1:1) are indicated by the black color code. Points referred to the same gene or similar functions are clustered together. After treated with 10 μM genistein for 1 and 3 h, Panc 1 cells show self-protection, because expressions of most genes during this period increase transiently. At 6 h, genes that show induction or depression are almost one to one. At 12 h, most genes are depressed.

saturase), DNA ligase III, and Rad (Ras-related associated with diabetes). There were also down-regulation in 18s and 28s rRNA levels.

We used real-time PCR analysis to confirm the changes in gene expression observed using the microarray assay. We found that real-time PCR analysis showed alterations in expression similar to those observed in the microarray assay for a number of genes (Fig. 3), yet the increase in change in expression levels was not exactly the same between the 2 assays.

## DISCUSSION

The present study is, to our knowledge, the first to examine the effect of a physiologically relevant concentration of genistein on gene expression using microarray analysis. Many researchers choose 50 μmol/L because lower doses of genistein did not cause observable changes in cell proliferation. However, 10 μmol/L is the high end of physiologically achievable genistein, so we chose to carry out a microarray analysis of cells exposed to this level.

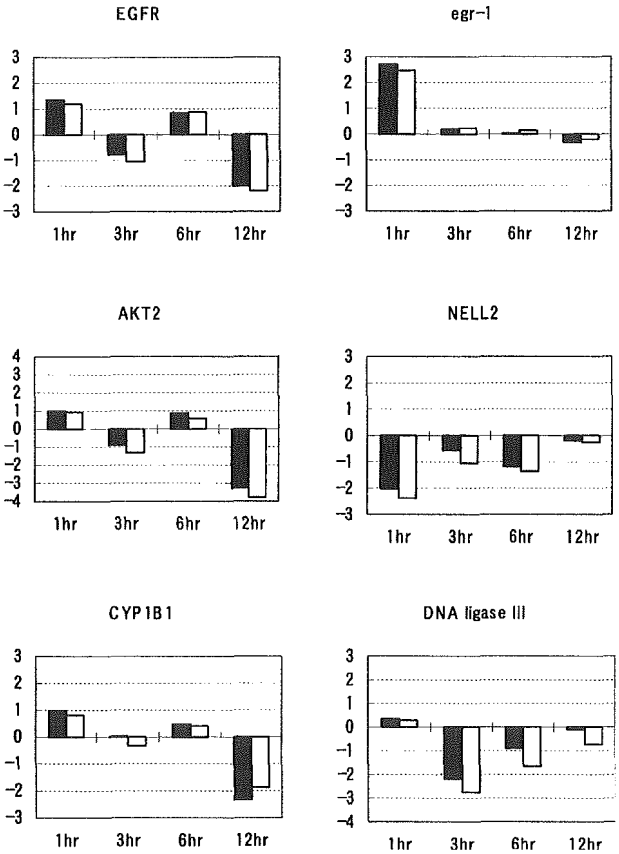


**FIGURE 3.** The real-time PCR analyses (▨) for the checked 6 genes were in agreement with the microarray data (■). The same RNA used in microarray is used in the real-time PCR. The y-axis indicates the log 2 transformed ratio of mRNA expression, which was compared with the vehicle-treated control group. The fluctuations of mRNA expression in Panc 1 cells treated with 10 μmol/L genistein for 1, 3, 6, and 12 hours are in these 2 different analytic methods, although the increase in change in expression levels is not exactly the same.

In tissue culture experiments, the condition of cells is critical since subtle growth differences can greatly influence gene expression profiles. Hughes et al[12] identified a number of transcripts that exhibited inherent fluctuation in isogenic untreated yeast cultures that appeared to have no phenotypic differences. Taking this into account, only genes that showed more than a fourfold change in expression by genistein were chosen for further analysis in the present study.

We found that genistein altered the expression of a number of genes known to be involved in the epidermal growth factor pathway, namely EGF-R, egr-1, AKT2, CYP1B1, and NELL2.

Genistein is a protein tyrosine kinase inhibitor. Tyrosine kinase activity of EGF-R is directly responsible for most cellular events mediated by EGF.[13] EGF-R is overexpressed in many malignancies, including pancreatic cancer, from which Panc 1 cells are derived. In breast cancer, intrinsic or acquired resistance to antiestrogens is often associated with elevated expression of EGF-R.[14] Dalu et al[15] found that genistein inhibited EGF-R expression in the rat dorsolateral prostate.

AKT2 can be activated by EGF, and overexpression of AKT2 contributes to the malignant phenotype in a subset of human ductal pancreatic cancers.[16] AKT2 up-regulation can be considered a self-protective mechanism after exposure to stress stimuli.[17] Our observed lowering of AKT2 expression by genistein suggests that it disables protective mechanisms in cancer cells.

egr-1 is also an important member of the EGF signaling cascade.[18] egr-1 gene expression has been monitored in many cell types in response to mitogens[19] and has also been connected with development of human cancers. Overexpression of egr-1 has been observed in the majority of human prostate cancer.[20] In our study, the expression profile of egr-1 matched the reported immediate early transcription of egr-1,[21] indicating that the microarray chip hybridization data concur with data generated using other methods. This conclusion is also supported by the expression profiles of FOS and FOSB in the current study, which match previous reports showing they are usually induced within 15 minutes and became undetectable after 1 hour.[22]

NELL2 contains EGF-like repeats and is a member of the epidermal growth factor gene family.[23] Others have shown NELL2 mRNA is abundantly expressed in Burkitt lymphoma, Raji cells, and colorectal adenocarcinoma SW480 cells.[24] Our observation that genistein inhibited NELL2 expression would likely result in decreased EGF signaling.

A role for cytochrome P-450 has been identified in the EGF-R signaling pathway.[25] Cells with active P-450 demon-

strated marked increases in both the extent and sensitivity of DNA synthesis in response to EGF. CYP1B1 belongs to the multigene family cytochrome P-450, which can influence the response of established tumors to anticancer drugs by metabolizing those drugs.[26] CYP1B1 shows increased expression in a wide range of human tumors, including breast and colon cancers and is specifically located in tumor cells.[27] Cytochrome P-450 can deactivate a wide variety of environmental chemicals and can thus can be considered as a self-protecting mechanism. Inhibition of CYP1B1 expression further suggests genistein can disable cancer cell protective mechanisms.

In addition to repression of a number of genes related to EGF signaling, we also observed that genistein inhibited expression of DNA ligase III, which plays an important role in DNA replication, recombination, and repair. After exposure to DNA-damaging agents, such as topoisomerase inhibitor, cell death signals are initiated. Genistein has been reported to inhibit topoisomerase II activity both in vitro and in vivo.[28,29] In addition to its structural role in restoring the integrity of the nuclear genome, DNA ligase III also plays an important role in fine-tuning the trigger point of the cell death cascade.[30] Our observation that genistein inhibited DNA ligase III gene expression suggests that genistein may block DNA replication, recombination, and repair in cancer cells.

In human breast cancer and melanoma cells, Rad acts to increase serum-stimulated DNA synthesis.[31] Although a decrease in Rad expression may decrease DNA synthesis, it increases the ability of cells to recruit glucose, which facilitates cancer growth.[32] However, Boros et al[33] reported that genistein could shift glucose carbons from cell proliferation–related structural and functional macromolecules (eg, RNA, DNA), which are synthesized through nonoxidative pathways, to direct oxidative degradation of glucose and thus diminished proliferation and survival of pancreatic adenocarcinoma cells in culture. Inhibiting the formation of ribose from glucose blocks ribosome formation and is one of the important underlying mechanisms by which genistein regulates tumor cell growth.[34] Consistent with those findings, the present study showed that genistein lowered levels of 18s and 28s rRNA after 12 hours. Lower 18s and 28s rRNA levels would not only reduce protein synthesis in general but also enhance the effect of genistein-lowering levels of specific mRNA species.

SCD overexpression is associated with genetic predisposition to hepatocarcinogenesis in mice and rats.[35] Overexpression of SCD has also been reported in rat mammary carcinomas, and sterculic acid, an SCD activity inhibitor, inhibits rat mammary carcinogenesis.[36] The possibility of SCD involvement in mammary carcinogenesis is strengthened by a case-control study suggesting a decreased risk of breast cancer in women with low SCD enzyme activity.[37] High SCD activity has been implicated in a wide range of disorders including diabetes, atherosclerosis, obesity, and viral infection. Our observation that genistein lowered SCD expression might explain the difference in the incidence of these diseases between Asian and Western populations.[38,39]

IL-8 has recently been shown not only to be overexpressed in various human cancers and cancer cell lines but also to contribute to human cancer progression.[40] Elevated IL-8 secretion may not only directly stimulate tumor cell proliferation but may also support tumor mass expansion via direct or indirect induction of tumor vessel formation.[41] Although IL-8 is associated with cancer progression, here we found that IL-8 gene expression was up-regulated about fivefold after 3 hours genistein treatment. This may explain why physiological levels of genistein can stimulate growth of solid tumors.[42] Thus, it appears genistein may be useful in preventing carcinogenesis but not useful as a chemotherapeutic agent for solid tumors.

In conclusion, the current data suggest genistein may inhibit carcinogenesis in several ways. The most obvious way is by interfering with the EGF-R signaling pathway. In addition, genistein appears capable of disabling cancer cell self-protective mechanisms. Furthermore, genistein may inhibit carcinogenesis by inhibiting DNA repair mechanisms. Finally, our data support findings indicating that genistein inhibits rRNA formation, which is an important mechanism by which genistein regulates tumor cell growth.

However, this work only addressed to cancer cells in vitro. Any attempt to apply this conclusion to normal cells or in vivo should be made with caution. Further experiments focusing on those aspects are needed.

## REFERENCES


1. Goodman MT, Wilkens LR, Hankin JH, et al. Association of soy and fiber consumption with the risk of endometrial cancer. *Am J Epidemiol.* 1997; 146:294–305.
2. Uckun FM, Messinger Y, Chen CL, et al. Treatment of therapy-refractory B-lineage acute lymphoblastic leukemia with an apoptosis-inducing CD19-directed tyrosine kinase inhibitor. *Clin Cancer Res.* 1999;5:3906–3913.
3. Kim H, Peterson TG, Barnes S. Mechanisms of action of the soy isoflavone genistein: emerging role for its effects via transforming growth factor β signaling pathways. *Am J Clin Nutr.* 1998;68(suppl):1418S–1425S.
4. Lamartiniere CA. Protection against breast cancer with genistein: a component of soy. *Am J Clin Nutri.* 2000;71:1705S–1707S.
5. Polkowski K, Mazurek AP. Biological properties of genistein. A review of in vitro and in vivo data. *Acta Pol Pharm.* 2000;57:135–155.
6. El-Zarruk AA, van den Berg HW. The anti-proliferative effects of tyrosine kinase inhibitors towards tamoxifen-sensitive and tamoxifen-resistant human breast cancer cell lines in relation to the epidermal growth factor receptors (EGF-R) and the inhibition of EGF-R tyrosine kinase. *Cancer Lett.* 1999;142:185–193.
7. Lian F, Bhuiyan M, Li YW, et al. Genistein-induced $G_2$-M arrest, $p21^{WAF1}$ upregulation, and apoptosis in a non-small-cell lung cancer cell line. *Nutr Cancer.* 1998;31:184–191.
8. Boros LG, Torday JS, Lim S, et al. Transforming growth factor β2 promotes glucose carbon incorporation into nucleic acid ribose through the nonoxidative pentose cycle in lung epithelial cells. *Cancer Res.* 2000;60: 1183–1185.
9. Peterson G. Evaluation of the biochemical targets of genistein in tumor cells. *J Nutr.* 1995;125:784S–789S.
10. Ju YH, Allred CD, Allred KF, et al. Physiological concentrations of dietary genistein dose-dependently stimulate growth of estrogen-dependent human breast cancer (MCF) tumors implanted in athymic nude mice. *J Nutr.* 2001;131:2957–2962.

11. Ju YH, Doerge DR, Allred KF, et al. Dietary genistein negates the inhibitory effect of tamoxifen on growth of estrogen-dependent human breast cancer (MCF-7) cells implanted in athymic mice. *Cancer Res.* 2002;62: 2474–2477.
12. Hughes TR, Marton MJ, Jones AR, et al. Functional discovery via a compendium of expression profiles. *Cell.* 2000;102:109–126.
13. Carpenter G, Wahl MI. The epidermal growth factor family. In: Sporn MB, Roberts AB, ed. *Peptide growth factors and their receptors I.* New York: Springer-Verlag; 1990:69–171.
14. Nicholson S. Epidermal growth factor receptor (EGFr) status associated with failure of primary endocrine therapy in elderly postmenopausal patients with breast cancer. *Br J Cancer.* 1988;58:810–814.
15. Dalu A, Haskell JF, Coward L, et al. Genistein, a component of soy, inhibits the expression of the EGF and ErbB/Neu receptors in the rat dorsolateral prostate. *Prostate.* 1998;37:36–43.
16. Ruggeri BA, Huang L, Wood M, et al. Amplification and overexpression of the AKT2 oncogene in a subset of human pancreatic ductal adenocarcinomas. *Mol Carcinog.* 1998;21:81–86.
17. Yuan ZQ, Feldman RI, Sun M, et al. Inhibition of JNK by cellular stress- and tumor necrosis factor α-induced AKT2 through activation of the NF κB pathway in human epithelial cells. *J Biol Chem.* 2002;277:29973–29982.
18. Kaufmann K, Thiel G. Epidermal growth factor and thrombin induced proliferation of immortalized human keratinocytes is coupled to the synthesis of egr-1, a zinc finger transcriptional regulator. *J Cell Biochem.* 2002;85:381–391.
19. Kaufmann K, Thiel G. Epidermal growth factor and platelet-derived growth factor induce expression of egr-1, a zinc finger transcription factor, in human malignant glioma cells. *J Neurol Sci.* 2001;1889:83–91.
20. Eid MA, Kumar MV, Iczkowski KA, et al. Expression of early growth response genes in human prostate cancer. *Cancer Res.* 1998;58:2461–2468.
21. Liu JW, Lacy J, Sukhatme VP, et al. Granulocyte-macrophage colony-stimulating factor induces transcriptional activation of Egr-1 in murine peritoneal macrophages. *J Biol Chem.* 1991;266:5929–5933.
22. Kovary K, Bravo R. Existence of different Fos/Jun complexes during the G0-to-G1 transition and during exponential growth in mouse fibroblasts: differential role of Fos proteins. *Mol Cell Biol.* 1992;12:5015–5023.
23. Watanabe TK, Katagiri T, Suzuki M, et al. Cloning and characterization of two novel human cDNAs (NELL1 and NELL2) encoding proteins with six EGF-like repeats. *Genomics.* 1996;38:273–276.
24. Kuroda S, Oyasu M, Kawakami M, et al. Biochemical characterization and expression analysis of neural thrombospondin-1-like proteins NELL1 and NELL2. *Biochem Biophys Res Commun.* 1999;265:79–86.
25. Chen JK, Wang DW, Falck JR, et al. Transfection of an active cytochrome P450 arachidonic acid epoxygenase indicates that 14.15-epoxyeicosatrienoic acid functions as an intracellular second messenger in response to epidermal growth factor. *J Biol Chem.* 1999;274:4764–4769.
26. Kivisto KT, Kroemer HK, Eichelbaum M. The role of human cytochrome P450 enzymes in the metabolism of anticancer agents: implications for drug interactions. *Br J Clin Pharmacol.* 1995;40:523–530.
27. Murray GI, Taylor MC, McFadyen MC, et al. Tumor-specific expression of cytochrome P450 CYP1B1. *Cancer Res.* 1997;57:3026–3031.
28. Markovits J, Linassier C, Fosse P, et al. Inhibitory effects of the tyrosine kinase inhibitor genistein on mammalian DNA topoisomerase II. *Cancer Res.* 1989;49:5111–5117.
29. Salti GI, Grewal S, Mehta RR, et al. Genistein induces apoptosis and topoisomerase II-mediated DNA breakage in colon cancer cells. *Eur J Cancer.* 2000;36:796–802.
30. Bordone L, Campbell C. DNA ligase III is degraded by calpain during cell death induced by DNA-damaging agents. *J Biol Chem.* 2002;277:26673–26680.
31. Zhu J, Tseng YH, Kantor JD, et al. Interaction of the Ras-related protein associated with diabetes Rad and the putative tumor metastasis suppressor NM23 provides a novel mechanism of GTPase regulation. *Proc Natl Acad Sci U S A.* 1999;96:14911–14918.
32. Moyers JS, Bilan PJ, Reynet C, et al. Overexpression of Rad inhibits glucose uptake in cultured muscle and fat cells. *J Bio Chem.* 1996;271: 23111–23116.
33. Boros LG, Bassilian S, Lim S, et al. Genistein inhibits nonoxidative ribose synthesis in MIA pancreatic adenocarcinoma cells: a new mechanism of controlling tumor growth. *Pancreas.* 2001;22:1–7.
34. Boros LG, Lapis K, Szende B. Wheat germ extract decrease glucose uptake and RNA ribose formation but increase fatty acid synthesis in MIA pancreatic adenocarcinoma cells. *Pancreas.* 2001;23:141–147.
35. Falvella FS, Pascale RM, Gariboldi M, et al. Stearoyl-Coa desaturase 1 (Scd1) gene overexpression is associated with genetic predisposition to hepatocarcinogenesis in mice and rats. *Carcinogenesis.* 2002;23:1933–1936.
36. Lu J, Pei H, Kaeck M, et al. Gene expression changes associated with chemically induced rat mammary carcinogenesis. *Mol Carcinog.* 1997; 20:204–215.
37. Chajes V, Hulten K, Van Kappel AL, et al. Fatty-acid composition in serum phospholipids and risk of breast cancer: an incident case-control study in Sweden. *Int J Cancer.* 1999;83:585–590.
38. Adlercreutz H, Mazur W. Phyto-oestrogens and Western diseases. *Ann Med.* 1997;29:95–120.
39. Barnes S. Evolution of the health benefits of soy isoflavones. *Proc Soc Exp Med.* 1998;217:386–392.
40. Xie KP. Interleukin-8 and human cancer biology. *Cytokine Growth Factor Rev.* 2001;12:375–391.
41. Yoshida S, Ono M, Shono T, et al. Involvement of interleukin-8, vascular endothelial growth factor, and basic fibroblast growth factor in tumor necrosis factor alpha-dependent angiogenesis. *Mol Cell Biol.* 1997;17: 4015–4023.
42. Helferich WG. Paradoxical effects of the soy phytoestrogen genistein on growth of human breast cancer cells in vitro and in vivo. *Am J Clin Nutr.* 1998;68:1524S–1525S.

# Reprogramming of human postmitotic neutrophils into macrophages by growth factors

Hiroto Araki, Naoyuki Katayama, Yoshihiro Yamashita, Hiroyuki Mano, Atsushi Fujieda, Eiji Usui, Hidetsugu Mitani, Kohshi Ohishi, Kazuhiro Nishii, Masahiro Masuya, Nobuyuki Minami, Tsutomu Nobori, and Hiroshi Shiku

**It is generally recognized that postmitotic neutrophils give rise to polymorphonuclear neutrophils alone. We obtained evidence for a lineage switch of human postmitotic neutrophils into macrophages in culture. When the $CD15^+CD14^-$ cell population, which predominantly consists of band neutrophils, was cultured with granulocyte macrophage–colony-stimulating factor, tumor necrosis factor-α, interferon-γ, and interleukin-4, and subsequently with macrophage colony-stimulating factor alone, the resultant cells had morphologic, cytochemical, and phenotypic features of macrophages. In contrast to the starting population, they were negative for myeloperoxidase, specific esterase, and lactoferrin, and they upregulated nonspecific esterase activity and the expression of macrophage colony-stimulating factor receptor, mannose receptor, and HLA-DR. $CD15^+CD14^-$ cells proceeded to macrophages through the $CD15^-CD14^-$ cell population. Microarray analysis of gene expression also disclosed the lineage conversion from neutrophils to macrophages. Macrophages derived from $CD15^+CD14^-$ neutrophils had phagocytic function. Data obtained using 3 different techniques, including Ki-67 staining, bromodeoxyuridine incorporation, and cytoplasmic dye labeling, together with the yield of cells, indicated that the generation of macrophages from $CD15^+CD14^-$ neutrophils did not result from a contamination of progenitors for macrophages. Our data show that in response to cytokines, postmitotic neutrophils can become macrophages. This may represent another differentiation pathway toward macrophages in human postnatal hematopoiesis. (Blood. 2004;103:2973-2980)**



## Introduction

One apparent characteristic of the hematopoietic system is that all types of mature cells with distinct functions are continuously replaced by cells derived from hematopoietic stem cells that reside mainly in the bone marrow and have the ability for self-renewal and multilineage differentiation.[1,2] In the process of differentiation, hematopoietic stem cells sequentially lose multilineage potential and generate lineage-committed progenitors with limited developmental capacity. Lineage-committed progenitors give rise to precursors that eventually differentiate into mature blood cells. After commitment to specific lineages, hematopoietic progenitor cells are incapable of producing mature cells of other lineages. For example, neutrophilic monopotent progenitors proliferate and differentiate into neutrophils, and progenitors restricted to a macrophage lineage cannot give rise to mature cells other than macrophages.

Several studies have focused on a lineage switch in the hematopoietic differentiation pathway. Boyd and Schrader[3] reported that murine pre–B-cell lines differentiate into macrophage-like cells in response to the demethylating drug, 5-azacytidine. B-lineage cells have been also shown to transit into neutrophils or natural killer (NK)/T-lineage cells.[4-8] Furthermore, the macrophage cell line differentiates into B-lineage cells.[9] Common lymphoid progenitors that exogenously express cytokine receptors or transcriptional factors develop myeloid lineage cells.[10-12] In addition to these lineage switches, lineage conversions within myeloid lineages have also been observed in experiments using cell lines and transformed cells. Enforced expression of transcriptional factors such as GATA-1 and PU.1 leads to the lineage switch of myeloid cells to cells with another myeloid phenotype.[12-17] These lineage switches include myeloid to megakaryocytic, myeloid to eosinophilic, myeloid to erythroid, and erythroid to myeloid conversions. The ectopic expression of PU.1 and C/EBP also results in the commitment of hematopoietic progenitors to an eosinophilic lineage.[18-20] With respect to normal primary cells, it has been reported that murine B-cell precursor cells acquire the potential to differentiate into macrophage-like cells when they are transferred to myeloid culture conditions.[21] Normal murine early T progenitor cells also generate macrophages in cultures supplemented with conditioned medium from a thymic stromal cell line or in the presence of cytokines.[22] Thus, normal murine lymphoid progenitors may retain the potential to differentiate into macrophages. Reynaud et al[23] reported that human cord blood–derived pro-B cells with $DJ_H$ rearrangements of the immunoglobulin (Ig) locus generate macrophages, NK cells, and T cells. However, it is unknown whether the lineage switch occurs in normal human mature hematopoietic cells.

We conducted research to determine whether normal postmitotic neutrophils are able to differentiate into other types of mature

From the Second Department of Internal Medicine, Mie University School of Medicine, Tsu, Japan; the Division of Functional Genomics, Jichi Medical School, Kawachi-cho, Japan; and the Blood Transfusion Service, Mie University Hospital, Tsu, Japan.

Submitted August 12, 2003; accepted December 18, 2003. Prepublished online as *Blood* First Edition Paper, December 30, 2003; DOI 10.1182/blood-2003-08-2742.

Supported in part by grants from the Japan Society for the Promotion of Science.

**Reprints:** Naoyuki Katayama, Second Department of Internal Medicine, Mie University School of Medicine, 2-174 Edobashi, Tsu, Mie 514-8507, Japan; e-mail: n-kata@clin.medic.mie-u.ac.jp.

The publication costs of this article were defrayed in part by page charge payment. Therefore, and solely to indicate this fact, this article is hereby marked "advertisement" in accordance with 18 U.S.C. section 1734.

cells. We found that human postmitotic neutrophils switched their differentiation program and acquired the features of macrophages in cultures supplemented with cytokines. These data support the possibility that postmitotic neutrophils commonly thought to be restricted to the neutrophilic differentiation pathway can become macrophages, and we argue that the lineage switch of human mature blood cells may, at least in part, be relevant to normal hematopoietic differentiation.

## Materials and methods

### Cytokines

Recombinant human macrophage colony-stimulating factor (M-CSF) and interferon-γ (IFN-γ) were purchased from R&D Systems (Minneapolis, MN). Recombinant human granulocyte macrophage–colony-stimulating factor (GM-CSF) was provided by Kirin Brewery (Tokyo, Japan). Recombinant human tumor necrosis factor-α (TNF-α) was a gift from Dainippon Pharmaceutical (Suita, Japan). Recombinant human interleukin-4 (IL-4) was provided by Ono Pharmaceutical (Osaka, Japan). Cytokines were used at the following concentrations: M-CSF, 100 ng/mL; IFN-γ, 25 IU/mL; GM-CSF, 10 ng/mL; TNF-α, 20 ng/mL; and IL-4, 10 ng/mL.

### Cell preparation

Peripheral blood was obtained from healthy Japanese donors given subcutaneous injections of granulocyte colony-stimulating factor (G-CSF) to harvest peripheral blood stem cells. Each donor gave written, informed consent. Peripheral blood mononuclear cells (PBMCs) were separated by centrifugation on Ficoll-Hypaque, washed with $Ca^{2+}$-, $Mg^{2+}$-free phosphate-buffered saline (PBS), and suspended in PBS with 0.1% bovine serum albumin (BSA) (Sigma Chemical, St Louis, MO). $CD15^+CD14^-$ cells were separated from PBMCs using CD14 and CD15 immunomagnetic beads (MACS; Miltenyi Biotec, Auburn, CA), according to the manufacturer's instructions. $CD14^+$ and $CD8^+$ cells were also separated from PBMCs using CD14 and CD8 immunomagnetic beads (MACS; Miltenyi Biotec), respectively. Healthy donors gave written, informed consent. The purity of $CD15^+CD14^-$, $CD14^+$, or $CD8^+$ cells exceeded 99%.

### Culture

Culture medium was RPMI 1640 (Nissui Pharmaceutical, Tokyo, Japan) supplemented with 2 mM L-glutamine, 50 U/mL penicillin, 50 μg/mL streptomycin, and 10% fetal bovine serum (FBS) (HyClone Laboratories, Logan, UT). $CD15^+CD14^-$ cells ($1 \times 10^6$/mL) were cultured with designated combinations of cytokines in a 24-well tissue culture plate (Nunc, Roskilde, Denmark) for 18 days. Half of the culture medium was replaced with fresh medium containing cytokines every 3 to 4 days. In some experiments, cells were plated with designated combinations of cytokines; on day 11 of culture, the cells were washed 3 times with PBS and replated in cultures containing M-CSF. $CD14^+$ and $CD15^+CD14^-$ cells ($1 \times 10^6$/mL) were cultured in the presence of M-CSF for 7 days. Viable cells were counted using trypan blue dye exclusion methods.

### Morphologic cell analysis

Cytospin preparations of freshly isolated and cultured cells were stained with May-Grünwald-Giemsa solution, myeloperoxidase (MPO) staining kit, and double-specific (naphthol AS-D chloroacetate esterase)/nonspecific (α-naphthyl butyrate esterase) esterase staining kit.

### Cell cycle analysis

Cell cycle analysis was made using the CycleTEST PLUS DNA Reagent Kit (Becton Dickinson, San Jose, CA) according to the manufacturer's instructions. Nuclear DNA content of freshly isolated $CD15^+CD14^-$ cells was analyzed on a FACSCalibur flow cytometer (Becton Dickinson) with ModFit software (Verity Software House, Topsham, ME). HPB-NULL cells (American Type Culture Collection, Manassas, VA) were used as a control. HPB-NULL cells were passaged every 24 hours for 3 days before use to minimize differences among experimental conditions.

### Flow cytometric analysis

The following murine or rat monoclonal antibodies (mAbs) were used: anti–CD14-phycoerythrin (anti–CD14-PE), anti–CD15-fluorescein isothiocyanate (anti–CD15-FITC), and anti–HLA-DR-PE (Becton Dickinson); anti–MPO-FITC (DAKO, Glostrup, Denmark); anti–lactoferrin-PE (Immunotech, Marseille, France); anti–*c-fms*/M-CSF receptor (anti–*c-fms*/M-CSFR) (Oncogene Research, Boston, MA); anti–mannose receptor-PE, anti–Ki-67-FITC, which reacts with a proliferation-associated nuclear antigen, antibromodeoxyuridine (anti-BrdU)–FITC, and anti–rat IgG2b-FITC (Becton Dickinson PharMingen, San Diego, CA). Rat immunoglobulin and FITC- or PE-labeled mouse immunoglobulin served as isotype control: rat IgG2b and mouse IgM-FITC (Becton Dickinson PharMingen); mouse IgG1-FITC, IgG1-PE, and IgG2a-PE (Becton Dickinson); and mouse IgG2b-PE (Coulter, Miami, FL).

For membrane staining, cells were incubated with mAbs for 30 minutes on ice and washed 3 times with PBS. Intracellular molecules were stained, using Cytofix/Cytoperm Kit (PharMingen, San Diego, CA). Cells were fixed for 20 minutes at 4°C with formaldehyde-based fixation medium, washed, resuspended in permeabilization buffer containing sodium azide and saponin, and stained with mAbs for 30 minutes at 4°C. Cells were washed with the permeabilization buffer and PBS. HPB-NULL cells were used as a positive control for Ki-67 staining. Flow cytometric analysis was performed, using a FACSCalibur flow cytometer. CellQuest software (Becton Dickinson) was used for data acquisition and analysis.

### BrdU and carboxyfluorescein diacetate succinimidyl ester (CFSE) labeling

For BrdU pulse labeling, freshly isolated and cultured cells ($1 \times 10^6$/mL) were incubated with 5 μg/mL BrdU (Sigma Chemical) for 40 minutes. The cells were washed with 0.1% BSA PBS, fixed with ice-cold 70% ethanol for 30 minutes at −20°C, and treated with 4 N HCl/0.5% Tween-20 at room temperature for 20 minutes for DNA denaturation. Acid was neutralized with 0.1 M $Na_2B_4O_7$. After washing with 0.1% BSA PBS, the cells were stained with FITC-conjugated anti-BrdU mAb. BrdU incorporation was analyzed using a FACSCalibur cytometer.[24] HPB-NULL cells served as a positive control for BrdU labeling.

Freshly isolated $CD15^+CD14^-$ cells ($1 \times 10^6$/mL) were labeled for 10 minutes at 37°C with 0.5 μM CFSE (Lambda, Graz, Austria) PBS, a cytoplasmic dye that is equally diluted between daughter cells, and were washed 3 times with 10% FBS RPMI 1640. CFSE-labeled $CD15^+CD14^-$ cells were cultured as described above. $CD8^+$ cells ($1 \times 10^6$/mL) were labeled with CFSE, washed with 10% FBS RPMI 1640, and cultured with T-cell expander beads (CD3/CD28 T-cell expander; DynalBiotech, Oslo, Norway) at a 1:3 bead-to-cell ratio for 5 days. CFSE-labeled freshly isolated and cultured cells were analyzed for fluorescence intensity using a FACSCalibur cytometer.[25]

### Microarray

Microarray assay was carried out as described.[26,27] Total RNA extracted from freshly isolated and cultured cells by the acid guanidinium method was used to synthesize double-stranded cDNA. Biotin-labeled cRNA was prepared from each cDNA by ENZO BioArray High-Yield RNA Transcript Labeling kit (Affymetrix, Santa Clara, CA), and hybridized with a GeneChip HGU133A microarray (Affymetrix) harboring more than 22 000 human probe sets. Hybridization, washing, and detection of signals on the arrays were performed using the GeneChip system (Affymetrix) according to the manufacturer's protocols. Fluorescence intensity for each gene was normalized on the basis of the median expression value of the positive control genes (Affymetrix; HGU133Anorm.MSK) in each hybridization. Every microarray analysis was repeated twice. Hierarchical clustering and Welch analysis of variance (ANOVA) of the data set were conducted by using GeneSpring 6.0 software (Silicon Genetics, Redwood, CA).

### Phagocytosis

Cultured cells ($2 \times 10^5$/mL) were incubated with FITC-dextran (40 000 molecular weight; Sigma Chemical) or FITC-latex beads (2 μm; Polysciences, Warrington, PA) for 1 hour at 37°C or 4°C. The uptake of FITC-dextran and FITC-latex beads was halted by the addition of cold 1% FBS PBS. After washing 3 times with 1% FBS PBS, cells were analyzed on a FACS flow cytometer.[28,29]

## Results

### $CD15^+CD14^-$ neutrophils generate macrophages

We isolated $CD15^+CD14^-$ cells from human blood samples. Portions of May-Grünwald-Giemsa–, MPO-, and double-specific/nonspecific esterase–stained preparations are presented in Figure 1A. The $CD15^+CD14^-$ cell fraction consisted of myelocytes, metamyelocytes, band cells, and segmented cells. Proportions of myelocytes, metamyelocytes, band cells, and segmented cells were 0.6% ± 0.2%, 9.2% ± 2.5%, 87.6% ± 2.5%, and 2.6% ± 0.4%, respectively ($n = 5$). $CD15^+CD14^-$ cells were positive for MPO and specific esterase but negative for nonspecific esterase. These staining patterns were found in all portions of cytospin preparations. We analyzed the cell cycle characteristics of $CD15^+CD14^-$ cells. All $CD15^+CD14^-$ cells were found in $G_1$ phase of the cell cycle (Figure 1B), supporting the notion that these cells are postmitotic. The expression of MPO, M-CSFR, lactoferrin, mannose receptor, and HLA-DR was assessed by phenotypic analysis (Figure 1C). $CD15^+CD14^-$ cells were $MPO^+$, M-$CSFR^-$, $lactoferrin^+$, mannose $receptor^-$, and $HLA\text{-}DR^-$, a finding compatible with typical features of mature neutrophils. $CD14^+$ cells were also prepared from blood samples. Cultures of $CD14^+$ cells in the presence of M-CSF gave rise to cells with small nuclei and intracytoplasmic vacuoles. These

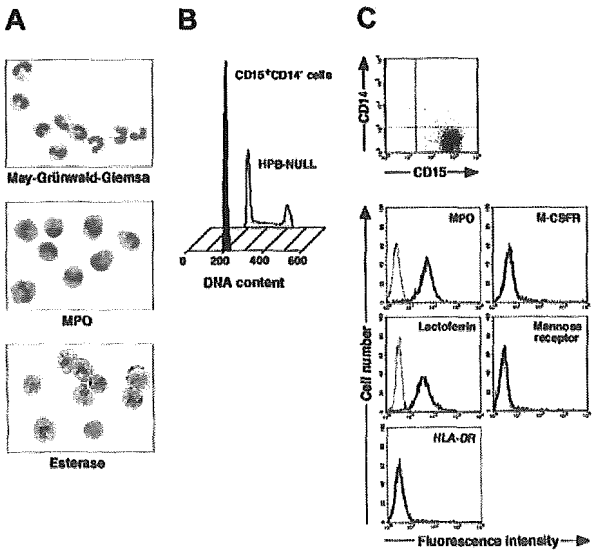


**Figure 1. Cytochemistry and phenotype of freshly isolated $CD15^+CD14^-$ cells.** (A) Photographs of May-Grünwald-Giemsa–, MPO-, and double-specific/nonspecific esterase–stained cytospin preparations; original magnification, × 400. (B) Nuclear DNA analysis of $CD15^+CD14^-$ cells was performed using a FACSCalibur flow cytometer. HPB-NULL cells were used as controls. Cell cycle distribution of HPB-NULL cells was as follows: with $G_1$ phase, 42.9%; S phase, 30.5%; and $G_2$/M phase, 26.6%. (C) The expression of CD15/CD14, MPO, M-CSFR, lactoferrin, mannose receptor, and HLA-DR was analyzed using a FACSCalibur flow cytometer. In the histograms, the thick and thin lines show the expression of the indicated molecules and isotype controls, respectively. Representative data from 5 independent experiments are shown.

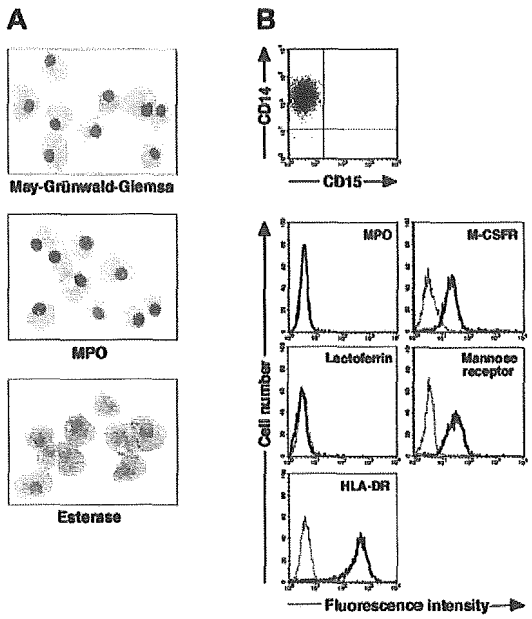


**Figure 2. Cytochemistry and phenotype of cells obtained from 7-day culture of freshly isolated $CD14^+$ cells with M-CSF.** (A) Photographs of May-Grünwald-Giemsa–, MPO-, and double specific/nonspecific esterase–stained cytospin preparations; original magnification, × 400. (B) The expression of CD15/CD14, MPO, M-CSFR, lactoferrin, mannose receptor, and HLA-DR was analyzed using a FACSCalibur flow cytometer. In the histograms, the thick and thin lines show the expression of the indicated molecules and isotype controls, respectively. Yield of cultured cells was 52.8% ± 9.8% ($n = 5$). Representative data from 5 independent experiments are shown.

cells showed nonspecific esterase activity but not MPO or specific esterase activity (Figure 2A), and they exhibited the phenotype of $CD15^-$ $CD14^+$, $MPO^-$, M-$CSFR^+$, $lactoferrin^-$, mannose $receptor^+$, and $HLA\text{-}DR^+$ (Figure 2B), which suggested that the resultant cells were macrophages. $CD15^+CD14^-$ cells were also cultured in the presence of M-CSF for 7 days. The yield was less than 2% of the starting population. Surviving cells retained the features of neutrophils (data not shown).

To determine whether postmitotic neutrophils have the potential to alter the lineage, we attempted to drive $CD15^+CD14^-$ cells to become cells of a monocyte/macrophage lineage, using cultures supplemented with cytokines. The combination of GM-CSF, M-CSF, TNF-α, and IFN-γ was chosen because GM-CSF, M-CSF, TNF-α, and IFN-γ are known to favor the differentiation of monocytes and their progenitors into macrophages.[1,30-36] Because M-CSF is a cytokine specific for, and late-acting in, a monocyte/macrophage lineage, we cultured $CD15^+CD14^-$ cells in the presence of GM-CSF, TNF-α, and IFN-γ for 11 days and subsequently replated the cells in cultures with M-CSF alone. On day 18 after the initiation of culture, cultured cells were harvested and characterized in morphologic, cytochemical, and phenotypic analyses. These cells had macrophage morphology (Figure 3A). Their MPO or specific esterase activity was not detected using light microscopy; however, the nonspecific esterase reaction was positive. CD14 expression was induced in a substantial, although not the entire, population of the resultant cells, but CD15 expression was completely lost (Figure 3B). When compared with freshly isolated $CD15^+CD14^-$ cells, the resultant cells did not entirely down-regulate MPO and lactoferrin yet they considerably up-regulated M-CSFR, mannose receptor, and HLA-DR. This culture condition yielded 1.8% ± 0.6% ($n = 5$) of the starting $CD15^+CD14^-$ cell population. These data suggest that GM-CSF, TNF-α, IFN-γ, and M-CSF allow $CD15^+CD14^-$ cells to become macrophages.

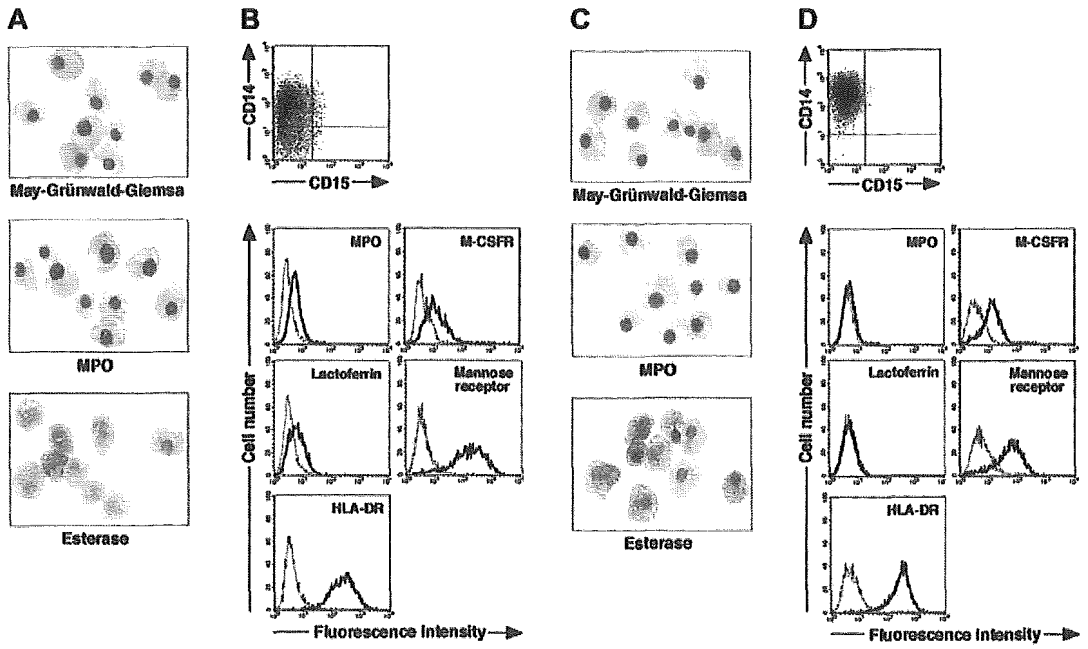


**Figure 3. Cytochemistry and phenotype of cells obtained from culture of freshly isolated CD15$^+$CD14$^-$ neutrophils.** (A-B) Freshly isolated CD15$^+$CD14$^-$ neutrophils were cultured with GM-CSF, TNF-α, and IFN-γ for 11 days, followed by additional 7-day culture with M-CSF alone. (C-D) Freshly isolated CD15$^-$CD14$^-$ neutrophils were cultured with GM-CSF, TNF-α, IFN-γ, and IL-4 for 11 days, followed by additional 7-day culture with M-CSF alone. (A,C) Photographs of May-Grünwald-Giemsa-, MPO-, and double specific/nonspecific esterase–stained cytospin preparations; original magnification, × 400. (B,D) The expression of CD15/CD14, MPO, M-CSFR, lactoferrin, mannose receptor, and HLA-DR was analyzed using a FACSCalibur flow cytometer. In the histograms, the thick and thin lines show the expression of the indicated molecules and isotype controls, respectively. Representative data from 5 independent experiments are shown.

Next, we searched for cytokine(s). The addition of cytokines to cultures would allow cells derived from CD15$^+$CD14$^-$ cells to acquire features more typical of macrophages. After testing several cytokines, we found that the appropriate conditions could be satisfied by supplementation with IL-4. When cultured with GM-CSF, TNF-α, IFN-γ, and IL-4 for 11 days and with M-CSF alone for 7 days, CD15$^+$CD14$^-$ cells gave rise to cells with morphologic characteristics of macrophages. The resultant cells were negative for MPO and specific esterase activities and positive for nonspecific esterase activity on cytospin preparations (Figure 3C). Phenotypic analysis showed that the resultant cells lacked CD15 and exclusively expressed CD14. MPO and lactoferrin were completely down-regulated, whereas the high levels of M-CSFR, mannose receptor, and HLA-DR expression were retained (Figure 3D), as in the macrophage phenotype induced from CD14$^+$ cells by M-CSF. Strikingly, the yield increased to 15.1% ± 3.6% (n = 5) of the starting CD15$^+$CD14$^-$ cell population. These observations unambiguously demonstrated a cytokine-induced lineage switch of postmitotic neutrophils to macrophages. We also cultured CD15$^+$CD14$^-$ cells in the presence of GM-CSF, TNF-α, IFN-γ, and IL-4 for 11 days and analyzed their phenotypes using flow cytometry. Cultured cells expressed neither CD15 nor CD14 (Figure 4A). MPO and lactoferrin were detected at low levels, whereas the expression levels of M-CSFR, mannose receptor, and HLA-DR were high (Figure 4B). These data suggest that the expression levels of molecules that characterize postmitotic neutrophils or macrophages are not simultaneously altered during this lineage switch program.

### Gene expression profiles of CD15$^+$CD14$^-$ neutrophils and macrophages

Given that the combination of cytokines consisting of GM-CSF, TNF-α, IFN-γ, IL-4, and M-CSF allowed for the generation of macrophages from CD15$^+$CD14$^-$ neutrophils, as determined by morphologic, cytochemical, and phenotypic analyses, we compared the gene expression profiles of freshly isolated CD15$^+$CD14$^-$ neutrophils, CD15$^+$CD14$^-$ neutrophil–derived macrophages, and CD14$^+$ cell–derived macrophages using high-density oligonucleotide microarrays. Because every microarray was repeated twice, the mean expression intensity was calculated for each gene and was used for the following analysis. Among our expression data set, first searched were the genes expressed abundantly in CD15$^+$CD14$^-$ neutrophils but not in CD14$^+$ cell–derived macrophages. Table 1 shows 10 such genes that had an expression level of more than 100 arbitrary units in CD15$^+$CD14$^-$ neutrophils and the highest ratio of the expression level between CD15$^+$CD14$^-$ neutrophils and CD14$^+$

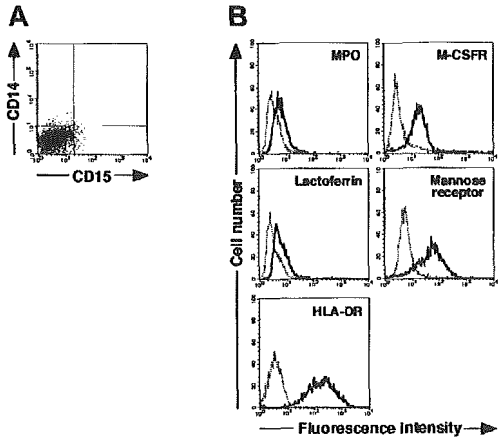


**Figure 4. Cytochemistry and phenotype of cells obtained from culture of freshly isolated CD15$^+$CD14$^-$ neutrophils with GM-CSF, TNF-α, IFN-γ, and IL-4 for 11 days.** (A) Expression pattern of CD15/CD14. (B) The expression of CD15/CD14, MPO, lactoferrin, M-CSFR, mannose receptor, and HLA-DR was analyzed using a FACSCalibur flow cytometer. In the histograms, the thick and thin lines show the expression of the indicated molecules and isotype controls, respectively. Representative data from 5 independent experiments are shown.